City of Morro Bay and
Cayucos Sanitary District

OFFSHORE MONITORING AND REPORTING PROGRAM

THIRD QUARTER RECEIVING–WATER SURVEY

SEPTEMBER 2016

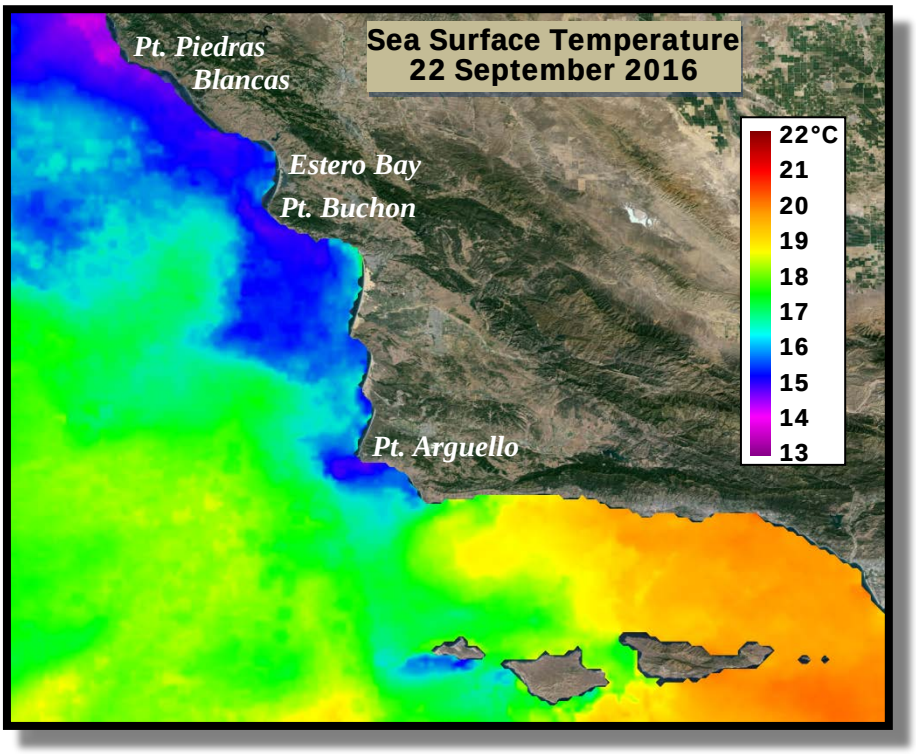

Marine Research Specialists
4744 Telephone Rd., Suite 3-315
Ventura, California 93003

Report to the

City of Morro Bay and
Cayucos Sanitary District

955 Shasta Avenue
Morro Bay, California 93442
(805) 772-6272

OFFSHORE MONITORING AND REPORTING PROGRAM

THIRD QUARTER RECEIVING–WATER SURVEY

SEPTEMBER 2016

Prepared by

Douglas A. Coats

Marine Research Specialists

4744 Telephone Rd., Suite 3-315
Ventura, California 93003

Telephone: (805) 644-1180
E-mail: Marine@Rain.org

October 2016

marine research specialists
4744 Telephone Rd., Suite 3-315 • Ventura, CA 93003 • 805-644-1180

Bruce Keogh
Wastewater Division Manager
City of Morro Bay
955 Shasta Avenue
Morro Bay, CA 93442

21 October 2016

Reference: Third Quarter Receiving-Water Survey Report – September 2016

Dear Mr. Keogh:

The attached report presents results from a quarterly receiving-water survey conducted on Tuesday, 20 September 2016. The survey was conducted in accordance with the requirements of the NPDES permit issued to the City and District for discharge of treated wastewater to Estero Bay. The report evaluated compliance with permit limitations and assessed the effectiveness of effluent dispersion. Quantitative analyses of continuous instrumental measurements and qualitative visual observations confirm that the wastewater discharge complied with the receiving-water limitations specified in the permit, and with the objectives of the California Ocean Plan.

The offshore measurements confirmed that the diffuser structure and treatment plant continued to operate at a high level of performance. The measurements delineated a diffuse discharge plume containing low organic loads within a highly localized region southwest of the discharge point. Dilution within the plume exceeded expectations based on modeling and outfall design criteria.

Please contact the undersigned if you have questions regarding the attached report.

Sincerely,

Douglas A. Coats

Douglas A. Coats
Program Manager

I certify under penalty of law that this document and all attachments were prepared under my direction or supervision in accordance with a system designed to assure that qualified personnel properly gather and evaluate the information submitted. Based on my inquiry of the person or persons who manage the system, or those persons directly responsible for gathering the information, the information submitted is, to the best of my knowledge and belief, true, accurate, and complete. I am aware that there are significant penalties for submitting false information, including the possibility of fine and imprisonment for knowing violations.

Bruce Keogh

Mr. Bruce Keogh
Wastewater Division Manager
City of Morro Bay

Date Oct 21, 2016

TABLE OF CONTENTS

LIST OF FIGURES

LIST OF TABLES

INTRODUCTION

The City of Morro Bay and the Cayucos Sanitary District (MBCSD) jointly own the wastewater treatment plant (WWTP) operated by the City of Morro Bay. In March 1985, Region IX of the U.S. Environmental Protection Agency (USEPA) and the Central Coast California Regional Water Quality Control Board (RWQCB) issued the first National Pollutant Discharge Elimination System (NPDES) permit to the MBCSD. The permit incorporated partially modified secondary treatment requirements for the plant's ocean discharge. The permit has been re-issued three times, in March 1993 (RWQCB-USEPA 1993ab), December 1998 (RWQCB-USEPA 1998ab), and January 2009 (RWQCB-USEPA 2009). The September 2016 field survey described in this report was the thirty-first receiving-water survey conducted under the current permit.

The NPDES discharge permit requires seasonal monitoring of offshore receiving-water quality with quarterly surveys. This report summarizes the results of sampling conducted on 20 September 2016. Specifically, this third-quarter survey captured ambient oceanographic conditions along the central California coast during the summer season. The survey's measurements were used to assess the discharge's compliance with the objectives of the California Ocean Plan (COP) and the Central Coast Basin Plan (RWQCB 1994) as promulgated by the receiving-water limitations specified in the NPDES discharge permit.

The monitoring objectives were achieved by empirically evaluating tabulations of instrumental measurements and standard field observations. In addition to the traditional, vertical water-column profiles, instrumental measurements were used to generate horizontal maps from high-resolution data gathered by towing a CTD[1] instrument package repeatedly over the diffuser structure. This allowed for a more precise delineation of the plume's lateral extent.

SURVEY SETTING

The MBCSD treatment plant is located within the City of Morro Bay, which is situated along the central coast of California halfway between Los Angeles and San Francisco. Effluent is carried from the onshore treatment plant through a 1,450-m long outfall pipe, which terminates at a diffuser structure on the seafloor 827 m from the shoreline within Estero Bay (Figure 1). The diffuser structure extends an additional 52 m toward the northwest from the outfall terminus and consists of 34 ports that are hydraulically designed to create a turbulent ejection jet that rapidly mixes effluent with receiving seawater upon discharge. Currently, six of the diffuser ports are kept closed, thereby improving effluent dispersion by increasing the ejection velocity from the remaining 28 ports distributed along a 42-m section of the diffuser structure.

Following discharge from the diffuser ports, additional turbulent mixing occurs as the buoyant plume of dilute effluent ascends through the water column. Most of this buoyancy-induced mixing occurs within a zone of initial dilution (ZID), whose lateral reach in modeling studies extends 15.2 m from the centerline of the diffuser structure. Beyond the ZID, energetic waves, tides, and coastal currents within Estero Bay further disperse the dilute effluent within the open-ocean receiving waters. Both vertical hydrocasts and horizontal tow surveys are conducted around the diffuser structure to assess the efficacy of the diffuser, to define the lateral extent of the discharge plume, and to evaluate compliance with the NPDES permit limitations.

[1] Conductivity, temperature, and depth (CTD)

Figure 1. Location of the Receiving-Water Survey Area

Near the diffuser, prevailing flow generally follows bathymetric contours that parallel the north-south trend of the adjacent coastline. Because of the rapid initial mixing achieved within 15 m of the diffuser structure, impingement of unmixed effluent onto the adjacent coastline, 827 m away, is highly unlikely. Nevertheless, in the event of a failure in the treatment plant's disinfection system, collection and analysis of water samples at the eight surfzone-sampling stations shown in Figure 1 would be conducted to monitor for potential shoreline impacts. These surfzone samples would be analyzed for total and fecal coliform, and enterococcus bacterial densities.

Areas of special concern, such as the Morro Bay National Estuary and the Monterey Bay National Marine Sanctuary, are not affected by the discharge because they are even more distant from the outfall location. For example, the southern boundary of the Monterey Bay National Marine Sanctuary is located 38 km to the north, while the entrance to the Morro Bay National Estuary lies 2.8 km south. The southerly orientation of the mouth of the Bay, and the presence of Morro Rock 2 km to the south, serve to further limit direct seawater exchange between the discharge point and the Bay (Figure 1).

SAMPLING LOCATIONS

As shown in Figure 2, the offshore sampling pattern consists of six fixed offshore stations located within 100 m of the outfall diffuser structure. The red ⊙ symbols in the Figure indicate the target locations of the sampling stations (Table 1). The stations are situated at three distances relative to the center of the diffuser structure, and lie along a north-south axis at the same water depth (15.2 m) as the center of the diffuser. Depending on the direction of the local oceanic currents at the time of sampling, the discharge may influence one or more of these stations. The up-current stations on the opposite side of the diffuser then act as reference stations. Comparisons between the water properties at these antipodal stations quantify departures from ambient seawater properties caused by the discharge and allow compliance with the NPDES discharge permit to be determined.

The finite size of the diffuser is an important consideration in the assessment of wastewater dispersion close to the discharge. Although the discharge is considered a "*point source*" for modeling and regulatory purposes, it does not occur at a single isolated point of infinitesimal size. Instead, the discharge is distributed along a 42 m section of the seafloor, and, ultimately, the amount of wastewater dispersion at a given point in the water column is dictated by its distance from the closest diffuser port, rather than its distance from the center of the diffuser structure. This "*closest approach*" distance can be considerably less than the centerpoint distance normally cited in modeling studies (last two columns of Table 1).

Another important consideration for compliance evaluation is the ability to determine the actual location of the measurements. Discerning small spatial separations within the compact sampling pattern only became feasible after the advent of Differential Global Positioning Systems (DGPS). The accuracy of traditional navigation systems such as LORAN or standard GPS is typically ±15 m, a span equal to half the total width of the ZID itself. DGPS incorporates a second signal from a fixed, land-based beacon that continuously transmits position errors in standard GPS readings to the DGPS receiver onboard the survey vessel. Real-time correction for these position errors provides an extremely stable and accurate offshore navigational reading with position errors of no more than 2 m, and often of sub-meter accuracy.

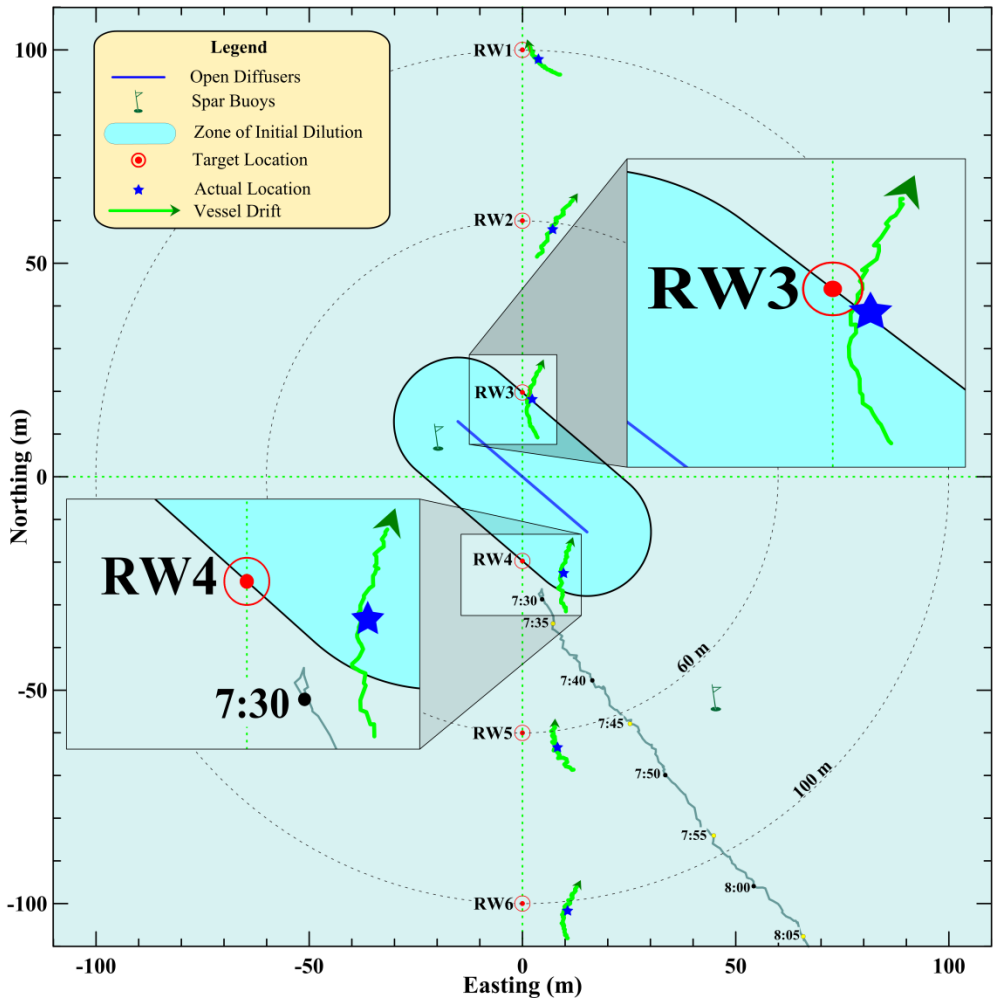

Figure 2. Station Locations

Table 1. Target Locations of the Receiving-Water Monitoring Stations

Station	Description	Latitude	Longitude	Center Distance[2] (m)	Closest Approach Distance[3] (m)
RW1	Upcoast Midfield	35° 23.253' N	120° 52.504' W	100	88.4
RW2	Upcoast Nearfield	35° 23.231' N	120° 52.504' W	60	49.4
RW3	Upcoast ZID	35° 23.210' N	120° 52.504' W	20	15.0
RW4	Downcoast ZID	35° 23.188' N	120° 52.504' W	20	15.0
RW5	Downcoast Nearfield	35° 23.167' N	120° 52.504' W	60	49.4
RW6	Downcoast Midfield	35° 23.145' N	120° 52.504' W	100	88.4

[2] Distance to the center of the open diffuser section
[3] Distance to the closest open diffuser port

During a diver survey in July 1998, the survey vessel's new DGPS navigation system, consisting of a Furuno™ GPS 30 and FBX2 differential beacon receiver, was used to precisely determine the position of the open section of the diffuser structure (MRS 1998) and establish the target locations for the receiving-water monitoring stations shown in Figure 2 and listed in Table 1. Presently, the use of two independent DGPS receivers onboard the survey vessel allows access to two separate land-based beacons for navigational intercomparison, ensuring extremely accurate and uninterrupted navigational reports.

Recording of DGPS positions at one-second intervals allows precise determination of sampling locations throughout the vertical CTD profiling conducted at the six individual stations, as well as during the tow survey. Knowledge of the precise location of individual CTD measurements relative to the diffuser is critical for accurate interpretation of the water-property fields. During vertical-profile sampling, the actual measurement locations rarely coincide with the target coordinates listed in Table 1 because winds, waves, and currents induce unavoidable horizontal offsets (drift). Even during quiescent metocean[4] conditions, the residual momentum of the survey vessel as it approaches the target locations can create perceptible offsets. Using DGPS however, these offsets can be quantified, and the vessel location can be precisely tracked throughout sampling at each station.

The downcasts during the September 2016 survey were conducted progressing from south to north, beginning with Station RW6. The magnitude of the drift at each of the six stations during the September 2016 survey is apparent from the length of the green tracklines in Figure 2. The tracklines trace the horizontal movement of the CTD as it was lowered to the seafloor at each station. Their lengths and offsets from the target locations reflect the overall station-keeping ability during the September 2016 survey.

The time it took the CTD to traverse the water column to the seafloor, which averaged 1 min 21 s, was consistent among stations, as was the lateral distance traversed by the instrument package during the downcasts, which averaged 13.6 m (Figure 2). The lateral movement of the CTD movement at any given time is typically determined by the complex interplay between the external influences of winds and currents, and the vessel's residual momentum immediately prior to each downcast. Lateral movement was greatest at Stations RW2, RW3, and RW4, where it exceeded 15.7 m. The drift at all stations had a northward component, in opposition to the southeastward current flow delineated by the drogued-drifter trajectory.[5] Northward vessel drift was, however, consistent with vessel transport by the prevailing winds, which were from the southwest.[6] The increased drift at Stations at RW2, RW3, and RW4 probably resulted from additional residual momentum of the vessel as it approached those stations from the south.

Regardless of the cause, detailed knowledge of the CTD's movement during downcasts is important for the interpretation of the water-quality measurements. Because the target locations for Stations RW3 and RW4 lie along the ZID boundary (viz, the red ⊙ symbols in the insets in Figure 2), knowledge of the CTD's location during the downcasts at those stations is especially important in the compliance evaluation. This is because the receiving-water limitations specified in the COP only apply to measurements recorded along or beyond the ZID boundary, where initial mixing is assumed complete.

[4] Meteorological and oceanographic conditions include winds, waves, tides, and currents.
[5] Refer to the drogued drifter track shown in Figure 3 later in this report.
[6] Refer to Table 4 later in this report.

During the September 2016 survey, only the deeper portion[7] of the data collected at Station RW3 was subject to a compliance assessment because the downcast began inside the ZID and traversed the ZID boundary at a depth of 8.5 m as it was transported toward the north.[8] Thus, only the data recorded below 8.5 m at Station RW4 were subject to the compliance analysis. This was the case even though the average location of the CTD data (blue star in the upper-right inset in Figure 2) was only 2.7 m from the target location (red target symbol in the inset).

Similarly, only the shallow portion[9] of the data collected at Station RW4 was subject to a compliance assessment because the cast began outside the ZID and traversed the ZID boundary at a depth of 3 m as it was transported toward the north.[10] Thus, only the data recorded below 2.5 m at Station RW4 were subject to the compliance analysis.

Compliance assessments notwithstanding, measurements acquired within the ZID lend valuable insight into the outfall's effectiveness at dispersing wastewater. For example, low dilution rates and concentrated effluent throughout the ZID would indicate potentially damaged or broken diffuser ports. Analysis of the outfall's operation over the past two and a half decades, however, demonstrates that it has maintained a high level of effectiveness in effluent dispersal. In fact, without the occasional measurements recorded within the ZID due to vessel drift, the extremely dilute discharge plume might remain undetected within all the vertical profiles collected during a given survey.

It has not always been possible to determine which measurements were subject to permit limits among hydrocasts near the ZID boundary, however. For example, prior to 1999 and before the advent of DGPS, CTD locations could not be determined with sufficient accuracy to establish whether the average station position was located within the ZID, much less how the CTD was moving laterally during the hydrocast. Because of these navigational limitations, sampling was presumed to occur at a single, imprecisely determined, horizontal location. Federal and state reporting of monitoring data still mandates identification of a single position for all of the CTD data collected at a particular station. Thus, for regulatory reporting, and for consistency with past surveys, the September 2016 survey also identifies a single sampling location for each station. These average station positions are identified by the blue stars in Figure 2, and are listed in Table 2 along with their distances from the diffuser structure.

Table 2. Average Position of Vertical Profiles during the September 2016 Survey

	Time (PDT)				Closest Approach	
Station	**Downcast**	**Upcast**	**Latitude**	**Longitude**	**Range[11] (m)**	**Bearing[12] (°T)**
RW1	9:19:34	9:20:55	35° 23.252' N	120° 52.502' W	87.1	13
RW2	9:16:40	9:17:58	35° 23.230' N	120° 52.499' W	50.3	26
RW3	9:13:52	9:15:09	35° 23.209' N	120° 52.502' W	**15.4[13]**	41
RW4	9:10:45	9:12:12	35° 23.187' N	120° 52.498' W	**11.0[13]**	210
RW5	9:07:46	9:09:06	35° 23.165' N	120° 52.499' W	50.8	188
RW6	9:04:23	9:05:48	35° 23.144' N	120° 52.497' W	88.7	183

[7] Below 8.5 m
[8] Refer to the upper right inset in Figure 2.
[9] Above 3 m
[10] Refer to the lower left inset in Figure 2.
[11] Distance from the closest open diffuser port to the average profile location
[12] Angle measured clockwise relative to true north from the closest diffuser port to the average profile location
[13] Some of the CTD measurements were located within the ZID boundary (refer to the insets in Figure 2).

OCEANOGRAPHIC PROCESSES

The trajectory of a satellite-tracked drogued drifter measured oceanic flow throughout the September 2016 survey (Figure 3). Modeled after the curtain-shade design of Davis et al. (1982) and drogued at mid-depth (7 m), a drifter has been deployed during each of the quarterly water column surveys conducted over the past two decades. In this configuration, oceanic flow rather than surface wind dictates the drifter's trajectory, which normally provides a good assessment of the plume's movement after discharge.

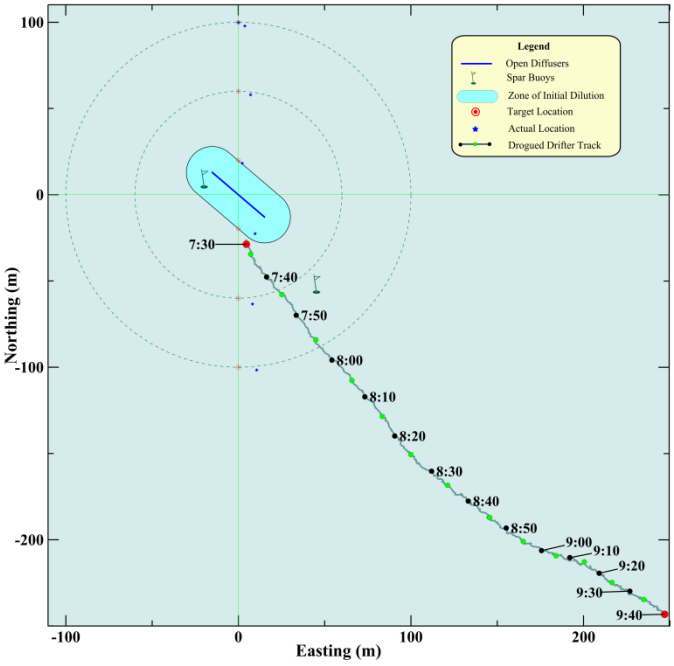

Figure 3. Drogued Drifter Trajectory

During the September 2016 survey, the drifter was deployed near the diffuser structure at 7:31 AM, and was recovered at 9:41 AM at a location 324 m southeast (132°T[14]) of its original release point (red dots in Figure 3). The nearly linear drifter track demonstrated that mid-depth oceanic current velocity was comparatively consistent throughout the survey. The uniform spacing between the green and black dots in Figure 3, which show the drifter's progress at five- and ten-minute intervals, indicates that flow speed varied little from the average speed of 4.2 cm/s.[15]

At that transport rate, effluent would have experienced a six-minute residence time within the ZID. However, the drifter trajectory only accurately captures the flow at mid-depth where the drifter's drogue is located. Occasionally, when the water column is moderately stratified, as was the case during the September 2016 survey, the flow can also vary significantly with depth. In some extreme cases, the flow near the seafloor can be in the opposite direction of the flow in the upper water column. In those cases of extreme vertical shear in the flow, the mid-depth flow direction measured by the drifter will not accurately predict the direction of plume transport. Such was the case during the September 2016, when flow within the benthic boundary layer above the seafloor was directed toward the north, while the flow in the surface mixed layer was toward the south. The mid-depth flow measured by the drifter was toward the southeast. This vertical change in flow direction explains why a deep plume signature was captured north of the diffuser structure at Stations RW2 and RW3, while mid-depth plume signatures were observed southwest of the diffuser structure at Station RW4.[16]

Oceanic flow near the survey area can be influenced by a variety of oceanographic processes, including tidal forcing, and upwelling, and by remote processes, such as large-scale along-shore pressure gradients, or the passing of large eddies embedded within the California Current. At any given time, one or more of these processes may dominate and control the observed flow field. For example, in the absence of other influences, the flood tide that prevailed during the September 2016 survey (Figure 4) tends to induce a

[14] Direction measured clockwise relative to true (rather than magnetic) north
[15] 0.081 kt
[16] Compare the reduced salinity near 11 m at Stations RW2 and RW3 (light green lines in Figure 8bc later in this report) with the reduced salinity between 4 m and 6 m at Station RW4 (Figure 8d)

weak northeastward (onshore) flow in the survey region. Because this direction is inconsistent with the observed flow, tidal forcing probably did not materially contribute during the September 2016 survey.

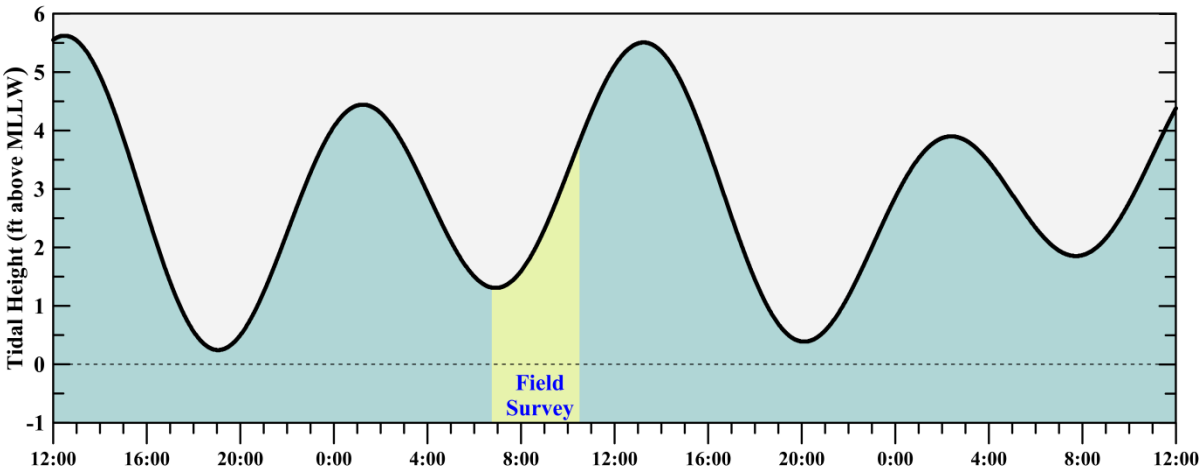

Figure 4. Tidal Level during the September 2016 Survey

Instead, as is usually the case along this section of coastline, currents within the survey area were largely determined by the prevailing wind field. Strong and steady northwesterly winds cause upwelling within the water column and produce a system of vertical countercurrents (Figure 5). In the upper water column, net wind-driven Ekman transport occurs at a 90º angle to the prevailing wind.[17] As a result, warm ocean waters within the surface mixed layer are driven offshore (southwestward) in response to the along-shore winds (toward the southeast). Near the coast, these warm surface waters are replaced by deep, cool, nutrient-rich waters that well up from below. The upwelled waters originate farther offshore and move shoreward (northwestward) along the seafloor as part of the upwelling process. Thus, upwelling establishes a vertical shear in flow within the survey area.

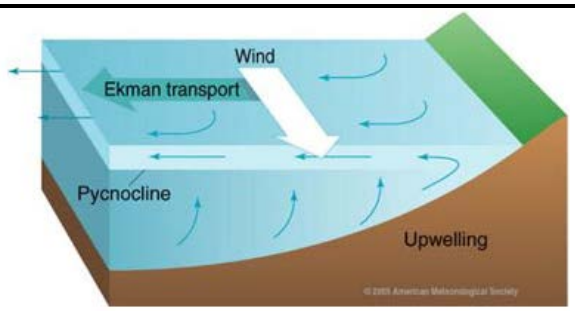

Figure 5. Schematic of Upwelling Processes

The onset of these upwelling-dominated processes begins with a rapid intensification of southeastward-directed winds along the central coast during late March and or early April as shown by the positive (blue) upwelling indices in Figure 6. This transition to more persistent southeastward winds is initiated by the stabilization of a high-pressure field over the northeastern Pacific Ocean. Clockwise winds around this pressure field drive prevailing northwesterly winds along the central California coast. The September 2016 survey was conducted well after the onset of this spring transition, and during a period when upwelling events were becoming less prevalent and their strength was declining relative to their peak intensity in July 2016 (see the last yellow diamond in Figure 6).

[17] http://oceanmotion.org/html/background/upwelling-and-downwelling.htm

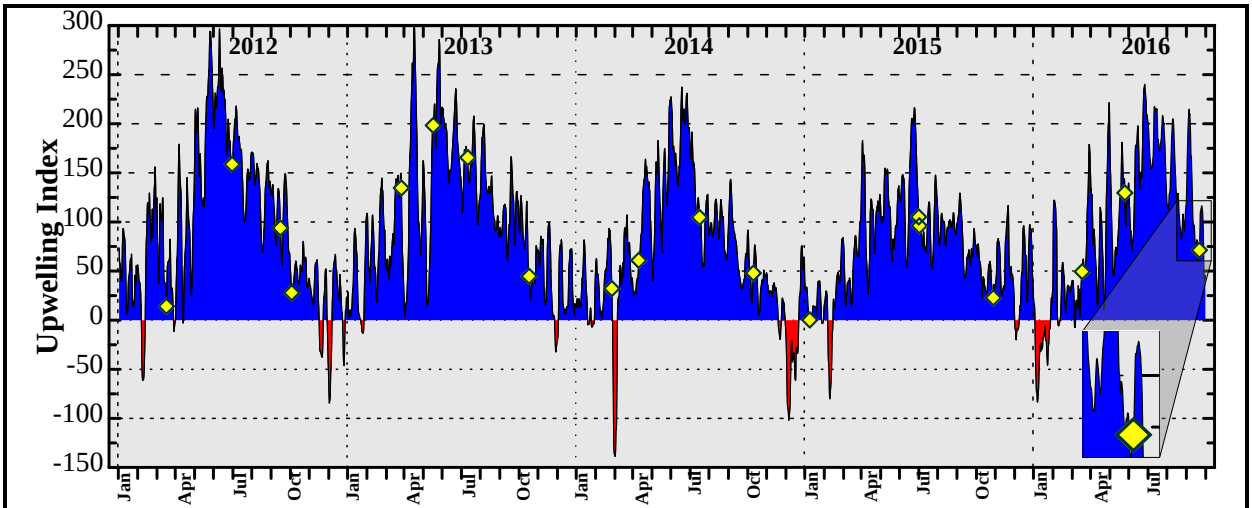

Figure 6. Five-Day Average Upwelling Index ($m^3/s/100$ m of coastline)

The nutrient-rich seawater that is brought to the sea surface near the coast by upwelling enables phytoplanktonic blooms that are the foundation of the productive marine fishery found along the central California coast. The vertical counterflow associated with persistent upwelling conditions also enhances vertical stratification of the water column. The influx of cold dense water at depth produces a thermocline that is commonly maintained throughout summer and into fall.

Some degree of upwelling is almost always present during offshore surveys (yellow diamonds in Figure 6). During winter, upwelling is typically weak, and occasionally downwelling events, indicated by the negative (red shaded) indices in Figure 6, occur when passing storms temporarily reverse the normal wind pattern and drive surface waters shoreward. As the surface waters approach the coastline, they downwell, producing nearly uniform seawater properties throughout the water column.

Because the September 2016 survey took place when upwelling was well underway, persistent upwelling winds were extant (see the last yellow diamond in Figure 6). These winds produced the typical spatial pattern of sea surface temperatures that are characteristic of upwelling processes within the central-coast region. This pattern was captured by the satellite image shown on the cover of this report. The image was recorded by infrared sensors on one of NOAA's polar orbiting satellites during a period of relatively cloudless skies two days after the survey. Cooler upwelled water is visually apparent along most of the entire south-central coastline (purple and dark blue shading).

The 5ºC cross-shore thermal contrast suggests fairly strong upwelling processes were present at the time the satellite image was recorded. However, weaker upwelling winds were present at the time of the survey, which occurred prior to a marked strengthening in upwelling winds. The inset in Figure 6 shows that northwesterly winds increased substantially (blue shading associated with the upwelling index) immediately after the survey (yellow diamond).

Observations of plume transport during the September 2016 survey were also consistent with the pattern of vertical countercurrents associated with upwelling (Figure 5). As described previously, the plume signature at depth was captured in the vertical profiles at Stations RW2 and RW3, where northeastward (onshore) currents would have transported the discharge plume. In contrast, a shallow plume signature

was observed at the southern ZID Station RW4, where southwestward (offshore) plume transport is consistent with upwelling-induced movement of near-surface waters. The southeastward trajectory of the drogued drifter, on the other hand, captured flow at an intermediate depth, which was not aligned with either of the cross-shore flow directions associated with upwelling.

Thus, the September 2016 survey captured upwelling conditions between strong northwesterly wind events. As a result, the water column was only moderately stratified, and the greatest stratification was measured at depth. As described later in this report, entrainment of markedly denser seawater near the seafloor in combination with turbulence generated by vertically sheared flow caused the plume to reach buoyant equilibrium at mid depth. Under other circumstances, the weaker stratification seen throughout the rest of the water column would not have been sufficient to trap the plume beneath the sea surface. When the plume mixes rapidly with particularly high-density seawater near the seafloor shortly after discharge, buoyancy forces within the effluent plume are diminished, and moderate stratification within the rest of the water column can trap the rising effluent plume beneath the sea surface, and curtail the initial dilution process. However, added turbulence from the vertically sheared flow can easily overcome the reduction in buoyancy-induced mixing resulting from a curtailed transit to the sea surface.

METHODS

The 38 ft F/V *Bonnie Marietta*, owned and operated by Captain Mark Tognazzini of Morro Bay, served as the survey vessel on Tuesday, 20 September 2016. Douglas Coats of Marine Research Specialists (MRS) supervised scientific operations as Chief Scientist, and provided data-acquisition and navigational support during the survey. He also assisted with the deployment and recovery of the CTD and drifter, and collected meteorological measurements at each station. Crewmember William Skok managed deck operations. Mr. Bruce Keogh, the MBCSD Wastewater Division Manager, and John Gunderlock, a Grade V operator at the WWTP, monitored operations onboard the vessel as client inspectors; and they also participated in data gathering by collecting Secchi Depth measurements at each station.

Auxiliary Measurements

Auxiliary measurements and observations were collected at each of the six stations after completion of the vertical profiling phase of the survey. Standard observations of weather and sea conditions, and beneficial uses, were augmented by visual inspection of the sea surface for floating particulates, oil sheens, and discoloration potentially related to effluent discharge. Other auxiliary measurements collected at each station included wind speeds and air temperatures measured with a handheld Holdpeak 866B Digital Thermo-Anemometer, and oceanic flow measurements made throughout the survey area using the aforementioned drogued drifter.

Additionally, at all six stations, a Secchi disk was lowered through the water column to determine its depth of disappearance. Secchi depths provide a visual measure of near-surface turbidity or water clarity. The depth of disappearance is inversely proportional to the average amount of organic and inorganic material suspended along a line of sight in the upper water column. As such, Secchi depths measure natural light penetration, which can be limited by increased suspended particulate loads from plankton blooms, onshore runoff, seafloor sediment resuspension, and wastewater discharge. They are also biologically meaningful because the depth of the euphotic zone, where most oceanic photosynthesis occurs, is limited to approximately twice the Secchi depth.

Instrumental Measurements

A Sea Bird Electronics SBE-19plusV2 Seacat CTD instrument package collected measurements of conductivity, temperature, light transmittance, dissolved oxygen (DO), pH, and pressure during the September 2016 survey. The six seawater properties used to assess receiving-water quality in this report were derived from the continuously recorded output from the CTD's probes and sensors. Although pressure-housing limitations confine the CTD to depths less than 680 m (Table 3), this is well beyond the maximum depth of the deepest station in the outfall survey. The entire CTD was returned to the factory in January 2015 for full calibration and servicing. The transmissometer and DO probe were returned to the manufacturer in January 2016 for further servicing, repair, and calibration.

Table 3. CTD Specifications

Component	Units	Range	Accuracy	Resolution
Housing (19p-1a; Acetron Plastic)	m	0 to 680	—	—
Pump (SBE 5P)	—	—	—	—
Pressure (19p-2h; Strain-Gauge)	dBar	0 to 680	±1.7	± 0.10
Conductivity	Siemens/m	0 to 9	± 0.0005	± 0.00005
Salinity	‰	0 to 58	± 0.004	± 0.0004
Temperature	ºC	–5 to 35	± 0.005	± 0.0001
Transmissivity (WETLabs C-Star)[18]	%	0 to 100	± 0.3	± 0.03
Oxygen (SBE 43)	% Saturation	0 to 120	± 2	—
pH (SBE 18)	pH	0 to 14	± 0.1	—

The precision and accuracy of the various probes, as reported in manufacturer's specifications, are listed in Table 3. Salinity (‰) was calculated from conductivity measurements reported in units of Siemens/m. Density was derived from contemporaneous temperature (°C) and salinity data, and was expressed as 1000 times the specific gravity minus one, which is a unit of sigma-T (σ_t).

Assessments of all three of the physical parameters (salinity, temperature, and density) helped determine the lateral extent of the effluent plume during the towing phase of the survey. Additionally, during the vertical-profiling phase, they quantified layering, or vertical stratification and stability of the water column, which determines the behavior and dynamics of the effluent as it mixes with seawater within and beyond the ZID. Data on the three remaining seawater properties, light transmittance (water clarity), hydrogen-ion concentration (acidity/alkalinity – pH), and dissolved oxygen (DO), further characterized the receiving waters, and were used to assess compliance with water-quality criteria. Light transmittance was measured as a percentage of the initial intensity of a transmitted beam of light detected at the opposite end of a 0.25-m path. Transmissivity readings are reported relative to 100% transmission in air, so the maximum theoretical transmission in (pure) water is expected to be 91.3%.

Before beginning the mid-depth tow survey at 7:45 AM, the CTD was deployed beneath the sea surface for eight minutes as the vessel was positioned to begin the first transect. Prior to deployment, the CTD package had been configured for horizontal towing with forward-looking probes. The protective cage around the CTD was fitted with a horizontal stabilizer wing and a depth-suppression weight was added to the towline to achieve near constant-depth tows.

[18] 25-cm path length of red (650 nm) light

Eight transects of mid-depth data were collected at an average depth of 7.2 m and an average speed of 1.83 m/s over the span of 35 minutes (blue-green lines in Figure 7). Subsequently, at 8:15 AM, eight additional passes were made with the CTD at an average depth of 4.2 m (orange lines). During this 30-minute shallow tow, vessel speed averaged 1.81 m/s. At the observed towing speeds and the 4 Hz sampling rate, at least 2.2 CTD measurements were collected for each meter traversed. This complies with the NPDES discharge permit requirement for minimum horizontal resolution of at least one sample per meter during at least five passes around and across the ZID at two separate depths, one within the surface mixed layer and one at mid-depth within the thermocline.

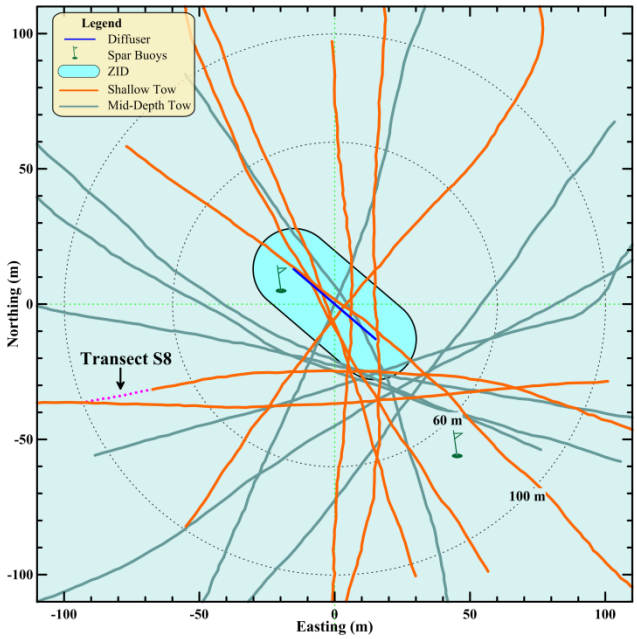

Figure 7. CTD Tracklines during the September 2016 Tow Surveys

Contemporaneous navigation fixes recorded onboard the survey vessel were adjusted for CTD setback and aligned with time stamps on the internally recorded CTD data. The resulting data for the six seawater properties were then processed to produce horizontal maps within the upper and sub-thermocline portions of the water column.[19]

At 8:48 AM, following completion of the last shallow transect, the CTD package was brought aboard the survey vessel and reconfigured for vertical profiling. The CTD was redeployed at 8:57 AM, and was held beneath the surface for seven minutes as the vessel was repositioned over Station RW6. The CTD was then raised to within 0.5 m of the sea surface and profiling commenced. The CTD was lowered at a continuous rate of speed to the seafloor. Measurements at all six stations were collected during a single deployment of the CTD package by towing it below the ocean surface while transiting between adjacent stations.

Quality Control

During the vertical-profiling and horizontal-towing phases of the survey, real-time data were monitored for completeness and range acceptability. Although real-time monitoring indicated the recorded properties were complete and within acceptable coastal seawater ranges,[20] subsequent post-processing revealed several events that impacted portions of the data, resulting in the adjustment or exclusion of these data prior to initiating the compliance analysis. Specifically, review of the tow data revealed that the CTD changed depth when the vessel executed a turn at the end of each transect. These vertical offsets in CTD depth are induced by changes in vessel speed and direction that are instituted to realign the vessel between each transect. Because of the complex interaction between turn radius, vessel speed, and CTD depth, the CTD's target depth cannot always be maintained at these times.

[19] Figures 9 and 10 later in this report

[20] Field sampling protocols employed during the survey generally followed the field operations manual for the Southern California Bight Study (SCBFMC 2002), which includes CTD cast-acceptability ranges listed in Table 2 of the manual.

Because the discharge-related anomalies used in the compliance analysis are identified by comparing the amplitudes of measurements acquired at the same depth level, the ability to resolve anomalies with statistical certainty is compromised when data from different depth levels are combined in the horizontal maps. This is particularly true whenever the water column is even moderately stratified, as was the case during the September 2016 survey.

However, the exclusion of portions of tow data did not adversely affect the compliance analysis. Only small portions of one transect (S8) exhibited depth offsets within the 100-m survey area (purple dotted lines in Figure 7). The remaining transects were long enough to fully encompass the 100-m survey area surrounding the diffuser structure. Specifically, the tow data that was included in the compliance analysis, shown by the solid orange and blue-green lines in Figure 7, met the permit monitoring requirement of at least five passes near the diffuser structure at each tow depth.

RESULTS

The third-quarter receiving-water survey was conducted on the morning of Tuesday, 20 September 2016. The receiving-water survey commenced at 7:30 AM with the deployment of the drogued drifter. Over the course of the ensuing two hours, offshore observations and measurements were collected as required by the NPDES monitoring program. The survey ended at 9:41 AM with the retrieval of the drogued drifter. Collection of required visual observations of the sea surface was generally unencumbered throughout the survey.

Auxiliary Observations

On the morning of 20 September 2016, skies were clear, with a sustained light onshore breeze out of the southwest. Auxiliary observations were collected beginning at 9:26 AM, after completion of the vertical profiling phase of the survey. During the subsequent 15 minutes, each station was re-occupied beginning with Station RW1, and sequentially progressing toward the south. During that time, wind direction and speed was variable, but winds were generally out of the southwest at an average speed of 3.5 kt (Table 4). A swell out of the northwest had a significant wave height of one-to-two feet. Air temperatures remained fairly constant and averaged 21.3°C, which was much warmer than the 15.4°C sea surface temperature.

There was no evidence of floating particulates, oil sheens, or any discoloration of the sea surface associated with the presence of wastewater constituents. There was no other visual indication of the presence of the discharge plume at or beneath the sea surface during the survey. Ambient light penetration through the water column was limited by an increased density of planktonic organisms within the upper half of the water column. During upwelling, nutrients carried upward into the euphotic zone are assimilated by phytoplankton, whose populations increase and, along with their associated zooplanktonic herbivores; their elevated densities reduce the transmittance of ambient light. At stations unaffected by the discharge during the September 2016 survey, plankton-induced increases in turbidity extended to a depth of approximately 6 m.

Because of this layer of increased turbidity, the Secchi disk consistently disappeared at a depth of 5 m as it was lowered through the water column at each station during the September 2016 survey (Table 4). The measured Secchi depth suggests indicates that a 10 m euphotic zone was present during the survey, and that ambient light only penetrated through the upper two-thirds of the water column and did not extend below the top of the deep thermocline that was present near 12 m at the time of the survey.

Table 4. Standard Meteorological and Oceanographic Observations

Station	Location[21] Latitude	Longitude	Diffuser Distance (m)	Time (PDT)	Air (°C)	Cloud Cover (%)	Wind Avg (kt)	Wind Dir (from) (°T)	Swell Ht/Dir (ft/°T)	Secchi Depth (m)
RW1	35° 23.252' N	120° 52.496' W	89.6	9:25:34	21.1	0	3.4	190	1-2 NW	5.0
RW2	35° 23.233' N	120° 52.500' W	54.2	9:28:54	22.6	0	3.3	280	1-2 NW	5.0
RW3	35° 23.206' N	120° 52.507' W	7.1	9:31:47	21.8	0	3.4	225	1-2 NW	5.0
RW4	35° 23.186' N	120° 52.494' W	11.4	9:33:56	20.8	0	3.4	190	1-2 NW	5.0
RW5	35° 23.168' N	120° 52.508' W	48.2	9:36:53	21.0	5	3.6	220	1-2 NW	5.0
RW6	35° 23.143' N	120° 52.503' W	92.0	9:39:16	20.5	0	3.6	220	1-2 NW	5.0

Because the Secchi-depth measurements were the same at all the stations, near-surface water clarity was not impacted by the presence of the plume, at least at the locations where the Secchi depth was measured. If anything, shallow measurements within the plume would be expected to increase Secchi depth because the rising effluent plume carried relatively clear deeper water into the shallow more-turbid mixed layer. Consistent with the invariant Secchi depths, there was no visual evidence of the plume signature at the sea surface at any time during the survey. Similarly, no evidence of floating particulates, oil sheens, or any discoloration of the sea surface was visually apparent that might be related to the presence of wastewater constituents.

Communication with plant personnel and subsequent review of effluent discharge properties on the day of the survey, confirmed that the treatment process was performing well at time of the survey. The 0.712 million gallons of effluent discharged on 20 September had a temperature of 24°C, a suspended-solids concentration of 46 mg/L, and a pH of 7.4. The 1.7 mg/L oil and grease concentration measured within effluent discharged on the day of the survey was below the method quantification threshold. The biochemical oxygen demand (BOD) within an effluent sample collected three days after the survey on 23 September was 45 mg/L.

Instrumental Observations

Data collected during vertical profiling were processed in accordance with standard procedures (SCCWRP 2002), and are collated at 0.5-m depth intervals in Table 5. Data collected during the September 2016 survey reflect moderately stratified conditions within Estero Bay indicative of a brief and partial relaxation in coastal upwelling following a prolonged period of intense upwelling winds (refer to the inset in Figure 6).

Upwelling of varying intensity occurs most of the year along the central California coast, with the strongest upwelling winds beginning in March or April and extending through the summer. The intensity of upwelling tends to decline into fall, although pulses of sustained northwesterly winds still occur. An intense upwelling event results in the rapid influx of dense, cold, saline water at depth and leads to a sharp thermocline, halocline, and pycnocline where temperature, salinity, and density change rapidly over a small vertical distance. Under these highly stratified conditions, isotherms crowd together to form a density interface that inhibits the vertical exchange of nutrients and other water properties, traps the effluent plume at depth, and reduces the initial dilution of the effluent plume.

[21] Locations are the vessel positions at the time the Secchi depths were measured. These depart from the CTD profile locations listed in Table 2 because they were collected after completion of the CTD profiling.

Table 5. Vertical Profile Data Collected on 20 September 2016

Depth (m)	Temperature (°C)						Salinity (‰)					
	RW-1	RW-2	RW-3	RW-4	RW-5	RW-6	RW-1	RW-2	RW-3	RW-4	RW-5	RW-6
0.5	15.411	15.450	15.389	15.374	15.393	15.323	33.488	33.501	33.493	33.494	33.496	33.494
1.0	15.402	15.420	15.392	15.385	15.381	15.305	33.493	33.494	33.494	33.494	33.493	33.493
1.5	15.391	15.390	15.376	15.358	15.373	15.270	33.493	33.493	33.494	33.492	33.494	33.492
2.0	15.346	15.350	15.334	15.343	15.307	15.234	33.491	33.492	33.492	33.493	33.491	33.493
2.5	15.301	15.322	15.303	15.326	15.252	15.225	33.490	33.491	33.491	33.492	33.490	33.494
3.0	15.286	15.310	15.291	15.307	15.215	15.222	33.491	33.492	33.491	33.490	33.490	33.494
3.5	15.282	15.298	15.281	15.229	15.201	15.220	33.491	33.491	33.491	33.475	33.492	33.495
4.0	15.274	15.286	15.269	15.136	15.192	15.217	33.489	33.491	33.491	33.460	33.493	33.496
4.5	15.265	15.280	15.259	15.116	15.180	15.208	33.490	33.491	33.491	33.461	33.493	33.496
5.0	15.259	15.274	15.205	15.118	15.171	15.189	33.491	33.491	33.488	33.466	33.493	33.496
5.5	15.245	15.269	15.154	15.088	15.168	15.164	33.491	33.492	33.487	33.466	33.494	33.495
6.0	15.169	15.253	15.126	15.043	15.165	15.144	33.488	33.491	33.488	33.461	33.495	33.495
6.5	15.127	15.230	15.097	15.061	15.136	15.097	33.488	33.489	33.488	33.477	33.494	33.492
7.0	15.105	15.199	15.058	15.052	15.100	15.055	33.488	33.489	33.482	33.483	33.493	33.490
7.5	15.073	15.144	15.059	15.042	15.035	15.026	33.489	33.488	33.485	33.485	33.486	33.487
8.0	15.038	15.119	15.053	14.985	14.979	15.005	33.489	33.488	33.486	33.479	33.481	33.486
8.5	15.004	15.103	14.981	14.944	14.917	14.951	33.490	33.488	33.469	33.477	33.473	33.479
9.0	14.962	15.101	14.938	14.933	14.914	14.912	33.488	33.489	33.462	33.475	33.479	33.478
9.5	14.921	15.073	14.927	14.928	14.906	14.896	33.487	33.489	33.462	33.476	33.485	33.483
10.0	14.867	14.990	14.886	14.929	14.896	14.876	33.484	33.485	33.449	33.482	33.487	33.486
10.5	14.821	14.923	14.825	14.919	14.879	14.870	33.484	33.478	33.439	33.486	33.487	33.488
11.0	14.795	14.837	14.808	14.895	14.847	14.767	33.484	33.462	33.443	33.487	33.487	33.483
11.5	14.790	14.817	14.808	14.875	14.713	14.693	33.485	33.472	33.447	33.487	33.480	33.483
12.0	14.802	14.809	14.822	14.847	14.611	14.564	33.486	33.482	33.469	33.487	33.481	33.481
12.5	14.806	14.761	14.813	14.704	14.501	14.425	33.489	33.485	33.479	33.482	33.479	33.481
13.0	14.752	14.601	14.772	14.564	14.432	14.340	33.485	33.481	33.483	33.482	33.481	33.483
13.5	14.683	14.393	14.662	14.390	14.381	14.305	33.483	33.480	33.481	33.478	33.482	33.485
14.0	14.583	14.208	14.511	14.330	14.310	14.278	33.482	33.479	33.481	33.483	33.485	33.487
14.5	14.312	14.137	14.375	14.306	14.162	14.161	33.476	33.482	33.481	33.485	33.482	33.486
15.0	14.217	14.120	14.238	14.153	14.074	14.095	33.483	33.485	33.482	33.482	33.486	33.488
15.5	14.115	14.109	14.112	14.076	14.057	14.070	33.483	33.487	33.483	33.485	33.488	33.490
16.0	14.142	14.076	14.149	14.063	14.053	14.059	33.508	33.489	33.517	33.488	33.490	33.491
16.5				14.063	14.055					33.498	33.498	

Table 5. Vertical Profile Data Collected on 20 September 2016 (continued)

Depth (m)	Density (σ_t)						pH					
	RW-1	RW-2	RW-3	RW-4	RW-5	RW-6	RW-1	RW-2	RW-3	RW-4	RW-5	RW-6
0.5	24.723	24.719	24.725	24.727	24.727	24.740	8.034	8.032	8.031	8.030	8.028	8.026
1.0	24.723	24.719	24.725	24.727	24.727	24.744	8.034	8.031	8.031	8.030	8.028	8.026
1.5	24.725	24.725	24.729	24.731	24.729	24.751	8.034	8.032	8.031	8.030	8.029	8.025
2.0	24.733	24.733	24.736	24.735	24.741	24.759	8.035	8.032	8.031	8.031	8.029	8.022
2.5	24.743	24.738	24.743	24.738	24.753	24.762	8.035	8.032	8.032	8.031	8.028	8.018
3.0	24.746	24.741	24.745	24.741	24.761	24.763	8.036	8.034	8.032	8.031	8.023	8.016
3.5	24.747	24.744	24.747	24.746	24.766	24.764	8.036	8.034	8.033	8.030	8.021	8.014
4.0	24.747	24.746	24.750	24.756	24.768	24.765	8.037	8.034	8.034	8.026	8.017	8.013
4.5	24.750	24.748	24.752	24.761	24.771	24.767	8.037	8.035	8.033	8.022	8.015	8.011
5.0	24.752	24.749	24.762	24.764	24.773	24.771	8.036	8.036	8.032	8.018	8.013	8.008
5.5	24.755	24.751	24.772	24.770	24.774	24.776	8.036	8.035	8.031	8.017	8.010	8.007
6.0	24.770	24.754	24.779	24.776	24.776	24.780	8.035	8.035	8.028	8.016	8.010	8.005
6.5	24.779	24.757	24.785	24.785	24.781	24.789	8.030	8.035	8.022	8.012	8.008	8.005
7.0	24.784	24.764	24.789	24.791	24.789	24.796	8.026	8.033	8.019	8.010	8.006	8.004
7.5	24.791	24.775	24.792	24.795	24.797	24.800	8.022	8.030	8.015	8.006	8.004	8.003
8.0	24.799	24.781	24.794	24.803	24.805	24.804	8.020	8.025	8.014	8.003	8.002	8.002
8.5	24.807	24.784	24.796	24.810	24.813	24.810	8.015	8.023	8.011	8.001	8.002	8.001
9.0	24.815	24.785	24.800	24.811	24.818	24.818	8.011	8.022	8.009	7.999	7.999	8.000
9.5	24.823	24.792	24.802	24.813	24.825	24.825	8.009	8.021	8.006	7.998	7.999	7.999
10.0	24.832	24.807	24.801	24.817	24.828	24.831	8.007	8.018	8.003	7.999	8.001	8.000
10.5	24.842	24.815	24.807	24.823	24.832	24.834	8.007	8.012	8.001	8.000	8.002	8.001
11.0	24.847	24.821	24.813	24.829	24.838	24.853	8.007	8.006	7.999	8.001	8.003	8.003
11.5	24.850	24.834	24.816	24.833	24.862	24.869	8.007	8.001	7.995	8.002	8.003	8.002
12.0	24.848	24.843	24.831	24.839	24.885	24.895	8.006	8.001	7.995	8.003	8.004	7.999
12.5	24.849	24.855	24.840	24.866	24.907	24.924	8.006	8.002	7.996	8.003	7.999	7.994
13.0	24.858	24.887	24.852	24.895	24.923	24.944	8.007	8.003	7.998	8.002	7.995	7.987
13.5	24.871	24.930	24.874	24.929	24.935	24.952	8.007	8.000	8.000	7.998	7.993	7.981
14.0	24.891	24.968	24.906	24.946	24.951	24.960	8.004	7.990	7.999	7.991	7.986	7.978
14.5	24.944	24.986	24.935	24.953	24.981	24.984	8.000	7.974	7.993	7.983	7.978	7.971
15.0	24.969	24.991	24.964	24.983	25.001	24.999	7.989	7.965	7.982	7.974	7.968	7.958
15.5	24.991	24.996	24.992	25.001	25.007	25.006	7.971	7.959	7.966	7.961	7.958	7.949
16.0	24.991	25.004	24.992	25.006	25.010	25.009	7.959	7.951	7.953	7.954	7.949	7.941
16.5				25.006	25.010					7.948	7.944	

Table 5. Vertical Profile Data Collected on 20 September 2016 (continued)

Depth (m)	Dissolved Oxygen (mg/L)						Transmissivity (%)					
	RW-1	RW-2	RW-3	RW-4	RW-5	RW-6	RW-1	RW-2	RW-3	RW-4	RW-5	RW-6
0.5	8.224	8.235	8.224	8.212	8.213	8.196	82.773	82.583	82.412	82.164	81.261	81.381
1.0	8.231	8.235	8.236	8.230	8.218	8.090	82.771	82.379	82.251	82.540	82.830	81.444
1.5	8.234	8.236	8.238	8.234	8.189	8.024	82.777	82.252	82.236	82.191	82.334	81.398
2.0	8.270	8.245	8.247	8.241	8.081	8.005	82.590	82.245	81.880	81.470	81.529	81.397
2.5	8.283	8.253	8.254	8.205	8.005	8.000	82.572	82.066	81.421	81.324	80.866	81.276
3.0	8.270	8.263	8.235	8.078	7.975	7.971	82.246	81.816	81.759	81.326	81.487	81.123
3.5	8.260	8.260	8.223	8.001	7.970	7.961	82.266	81.919	82.036	81.509	81.622	80.885
4.0	8.240	8.255	8.198	8.002	7.938	7.926	82.434	81.760	80.984	81.918	81.736	80.886
4.5	8.232	8.255	8.104	7.977	7.914	7.897	82.897	81.523	80.525	82.232	81.643	80.578
5.0	8.188	8.252	8.010	7.910	7.909	7.877	82.394	82.037	81.895	82.168	81.805	80.544
5.5	8.026	8.212	7.984	7.876	7.876	7.848	82.408	82.030	83.382	82.386	82.032	80.800
6.0	8.022	8.206	7.901	7.849	7.809	7.812	81.832	81.007	84.558	82.955	81.949	81.056
6.5	7.955	8.108	7.851	7.794	7.792	7.785	83.369	80.636	84.989	83.301	81.427	81.468
7.0	7.869	7.973	7.877	7.766	7.726	7.765	84.227	81.288	85.234	83.569	81.363	82.404
7.5	7.834	7.987	7.821	7.711	7.670	7.744	84.648	83.375	85.159	83.158	82.180	83.024
8.0	7.771	7.971	7.733	7.699	7.678	7.681	85.222	84.107	85.365	82.849	83.386	83.222
8.5	7.721	7.961	7.717	7.699	7.732	7.698	85.856	84.546	85.497	83.251	83.850	83.698
9.0	7.715	7.855	7.713	7.715	7.754	7.711	85.977	85.194	85.339	83.563	84.520	83.801
9.5	7.676	7.689	7.638	7.739	7.743	7.725	86.328	85.219	85.415	83.930	84.697	84.216
10.0	7.665	7.634	7.582	7.761	7.729	7.693	86.397	85.517	85.333	83.811	84.616	84.553
10.5	7.672	7.600	7.590	7.738	7.627	7.587	87.034	85.537	85.251	83.992	85.001	85.535
11.0	7.665	7.649	7.630	7.743	7.481	7.577	87.612	85.586	85.205	84.414	85.671	85.612
11.5	7.672	7.667	7.645	7.710	7.486	7.426	88.183	85.447	85.319	84.712	86.701	85.966
12.0	7.661	7.585	7.646	7.527	7.381	7.275	88.579	86.092	85.634	84.806	87.808	87.877
12.5	7.617	7.316	7.577	7.414	7.321	7.206	88.279	86.642	86.467	86.855	90.065	89.435
13.0	7.552	6.975	7.404	7.250	7.285	7.146	88.049	88.560	86.928	89.375	91.023	90.857
13.5	7.334	6.904	7.276	7.204	7.100	7.118	89.397	90.114	88.390	91.346	91.613	91.180
14.0	6.985	6.850	7.209	7.191	6.740	6.872	90.293	89.241	89.670	91.517	91.578	91.001
14.5	6.961	6.843	6.927	6.869	6.719	6.737	90.719	87.641	91.086	91.042	90.281	90.167
15.0	6.840	6.816	6.753	6.705	6.727	6.727	88.648	86.841	90.647	88.839	87.113	86.441
15.5	6.838	6.782	6.808	6.723	6.705	6.719	86.709	86.344	86.057	83.766	84.111	85.254
16.0	6.801	6.806	6.711	6.707	6.711	6.740	85.822	85.232	83.567	82.451	83.993	82.610
16.5				6.698	6.722					82.480	83.567	

If the upwelling winds are only of moderate strength, occur only briefly, or have not occurred recently; vertical mixing slowly erodes the sharp contrast between the surface and deep watermasses, and stratification appears as a more gradual vertical change in seawater properties that can extend throughout the water column. This was the case during the September 2016 survey when the sharply defined vertical transition zone produced by strong upwelling winds in prior days and weeks had begun to erode, resulting in vertical profiles that exhibited a more gradual change with depth (Figure 8). Absent are sharply defined interfaces where large changes in seawater properties occur within a small vertical extent; signatures that are normally indicative of strong, recent upwelling conditions. In contrast, the thermocline that was present during the September 2016 survey extended across most of the water column. Slightly enhanced vertical gradients were apparent between 10 and 14 m. They were located immediately above a deep watermass containing more uniform seawater properties that extended to the seafloor.

These gradual vertical changes reflect a transition from warm surface waters to a colder, saltier, nutrient-rich but oxygen-poor watermass that migrated shoreward along the seafloor as part of the upwelling process. This offshore watermass moved shoreward to replace nearshore surface waters that were driven offshore by Ekman transport from the prevailing northwesterly winds (Figure 5). The seawater properties of this deep watermass originate within the northward-flowing Davidson undercurrent that carried more saline and less oxygenated waters out of the Southern California Bight and northward along the central California coast.

These regional processes influenced the distribution of seawater properties within the survey area in a predictable manner; namely, seawater properties exhibited steadily increasing or decreasing values with depth that were determined by well-established physicochemical processes within ocean waters (Figure 8). In particular, temperature (red lines), DO (dark blue lines), pH (olive-colored lines) steadily decreased with increasing depth. These decreases were mirrored by a pycnocline, where density (black lines) steadily increased with depth. Because the deep offshore watermass that was transported shoreward had not been in recent direct contact with the atmosphere, biotic respiration and decomposition had depleted its DO levels (dark blue lines). Additionally, at depth, biotic respiration and decomposition produced carbon dioxide (CO_2), and in its dissolved state, the increased concentration of carbonic acid appears as a concomitant reduction in pH (olive-colored lines).

Meanwhile, within the euphotic zone, nutrient-rich seawater brought to the sea surface by the recent upwelling facilitated phytoplankton blooms that produced oxygen, consumed carbon dioxide (increasing pH), and decreased water clarity (light blue lines).[22] The increased plankton density within the upper water column caused a 9.5% decrease in transmissivity compared to the highest-clarity seawater that was encountered near a depth of 14 m. Below this deep localized maximum in transmissivity, water clarity again declined within the deep watermass due to naturally occurring resuspension processes associated with the seafloor. During upwelling, the shoreward transport of offshore waters along the seafloor occasionally generates increased turbulence and shear within a benthic nepheloid layer (BNL). These thin, transient, particle-rich layers form when lightweight flocs of detritus are resuspended by the turbulence generated from bottom currents. BNLs are a widespread phenomenon on continental shelves (Kuehl et al. 1996) and have been regularly documented in past surveys conducted within Estero Bay.

[22] During the September 2016 survey, the surface mixed layer extended from the sea surface to a depth of approximately 6 m, as delineated by the region of relatively uniform seawater properties in Figure 8.

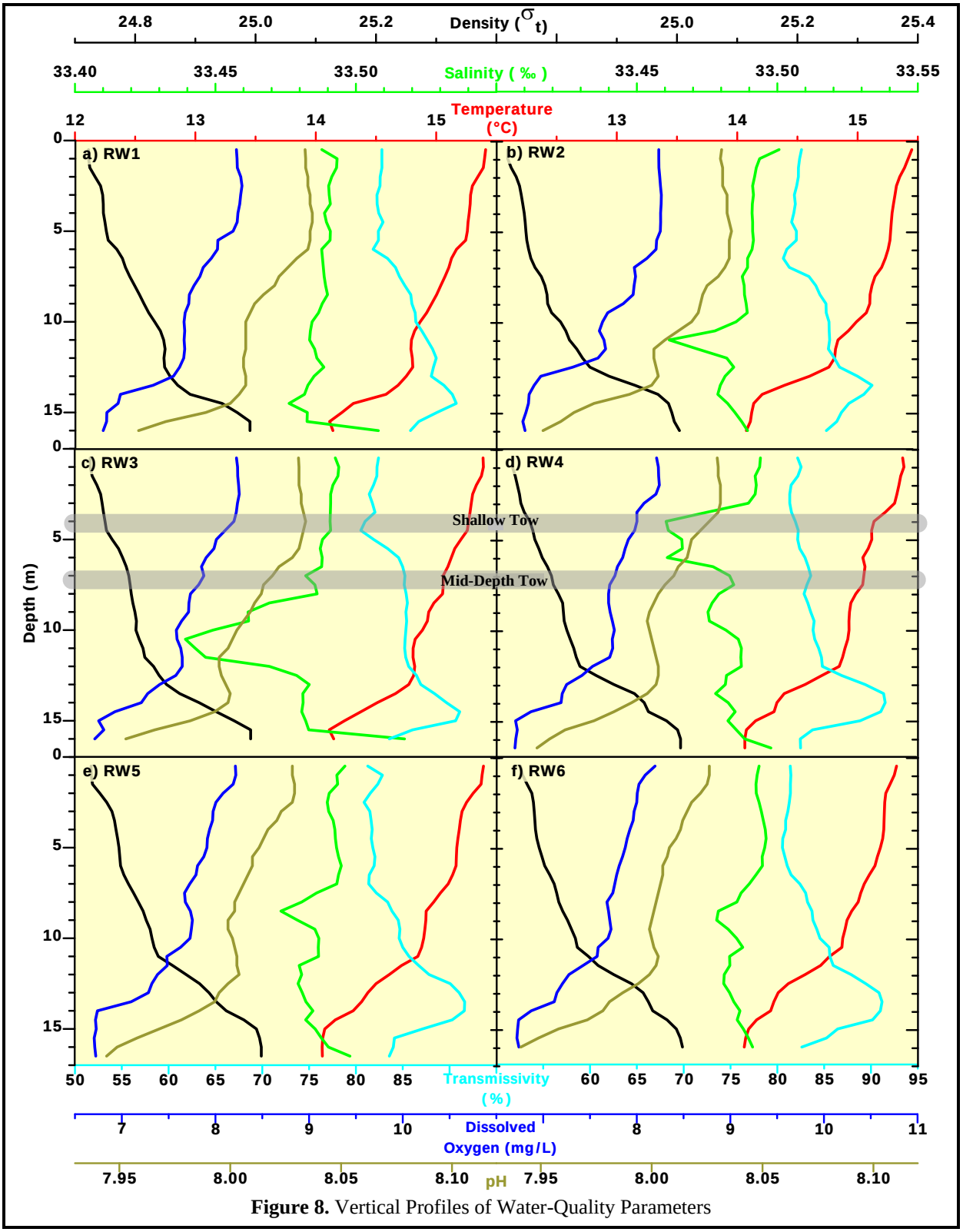

Figure 8. Vertical Profiles of Water-Quality Parameters

In addition to the influence of natural processes on the vertical profiles shown in Figure 8, several of the salinity profiles (green lines in Figure 8bcd) exhibit localized reductions that were caused by the presence of dilute effluent within the rising effluent plume. The strongest plume signature is apparent between 8 and 13 m at the northern ZID Station RW3 (green line in Figure 8c). At the station slightly to the north (RW2, Figure 8b), the amplitude of the salinity reduction was smaller and limited to a narrower depth range centered around 11 m. These data suggest that the plume signature was dissipating as it was carried northward by a deep current. However, the presence of a shallower salinity reduction, between 3 and 7m at the southern ZID Station RW4 (Figure 8d) indicates that the plume was transported in the opposite direction after rising into the upper water column.

Because of this apparently strong vertical shear in the flow, and because the tow surveys were conducted in the upper water column (thick shaded lines in Figure 8cd), the tow data did not capture the deep salinity reductions seen near 11 m north of the diffuser structure at Stations RW2 and RW3. Instead, the presence of highly diluted effluent was only delineated by the mid-depth tow data at a location southwest of the diffuser structure. The presence of dilute wastewater constituents was confirmed by the very weak salinity reductions that were observed over a limited area just beyond the ZID in the mid-depth tow data (green and red shading in Figure 9b). Very slight reductions in temperature, DO, and pH (Figure 9aef), and increases in density and transmissivity (Figure 9cd) coincided spatially with the salinity signature, and further confirmed the presence of the plume at that location.

Much larger amplitude anomalies in all the seawater properties except salinity were delineated in the northeast quadrant of the survey area (Figure 9acdef). However, these large anomalies could not have been induced by the presence of wastewater constituents because they did not coincide spatially with a perceptible salinity reduction (Figure 9b). Instead, this large pool of cold dense seawater probably resulted from a localized upwelling event that brought deep seawater characteristics upward in the water column.

Neither the pool of upwelled seawater nor effluent constituents associated with the rising effluent plume were apparent in the data collected during the shallow tow survey (Figure 10). Although very slight lateral changes were apparent in the shallow tow data, they tended to be randomly distributed within the survey area and generally did not coincide spatially with one another. Instead, they probably reflect natural variability in the lateral distribution of ambient seawater properties. Furthermore, the absence of a clear salinity reduction associated with the effluent plume southwest of the diffuser structure (Figure 10b) indicates that the rising plume had become trapped beneath the sea surface at some depth below the 4.2 m shallow tow depth, and at or above the 7.2 m mid-depth tow.

Although the localized salinity reduction found within the mid-depth tow data was indicative of the presence of dilute effluent constituents (Figure 9b), the plume signatures in other seawater properties found at the same locale were not caused by the presence of effluent itself. Instead, they were generated by the entrainment of ambient seawater at depth. The properties of that deep seawater were carried upward through the water column by the rising plume. Because the properties of the deep seawater differed from those of the ambient seawater in the upper water column, they generated lateral anomalies when they were juxtaposed by the rising plume.

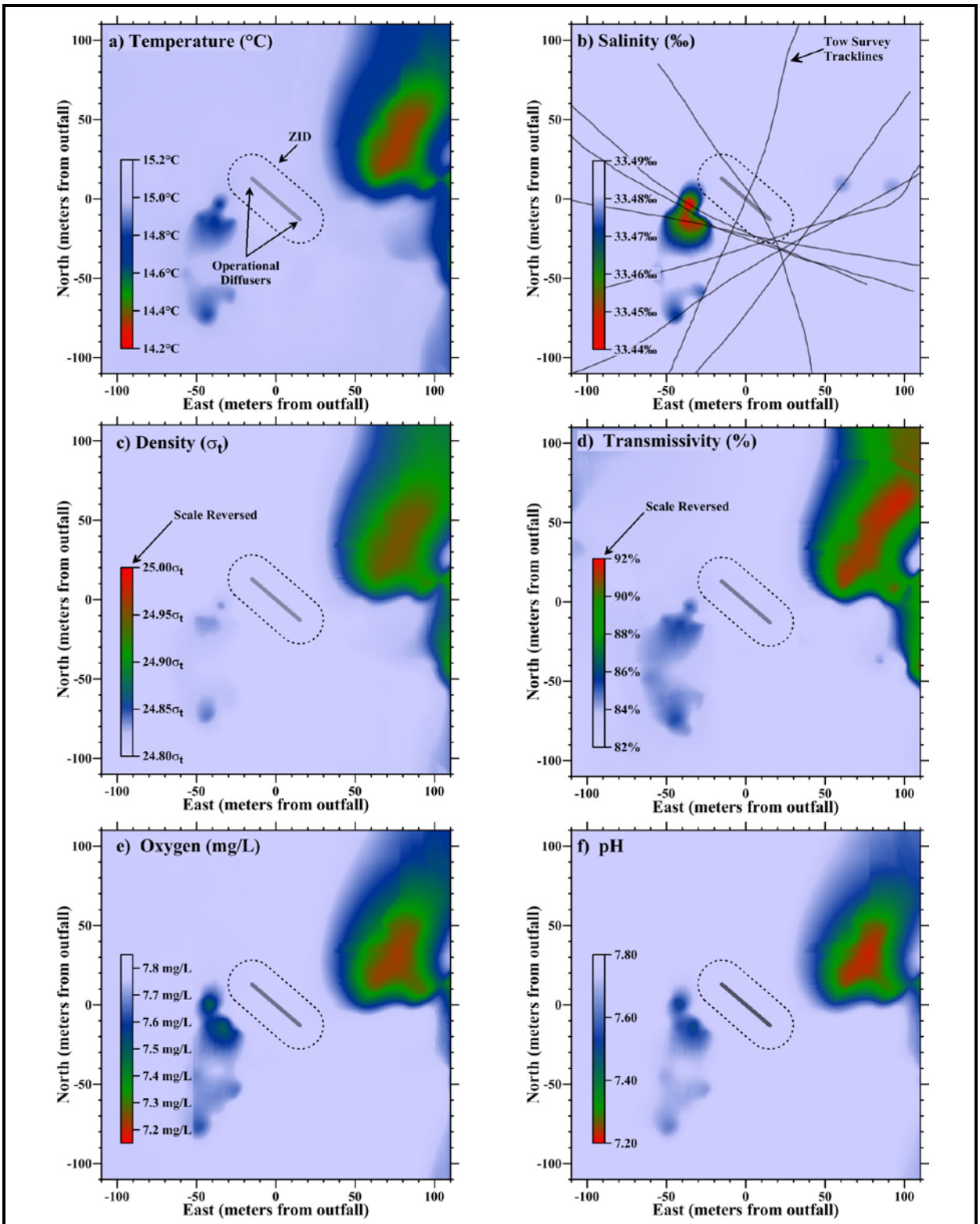

Figure 9. Horizontal Distribution of Mid-Depth Water-Quality Parameters 7.2 m below the Sea Surface

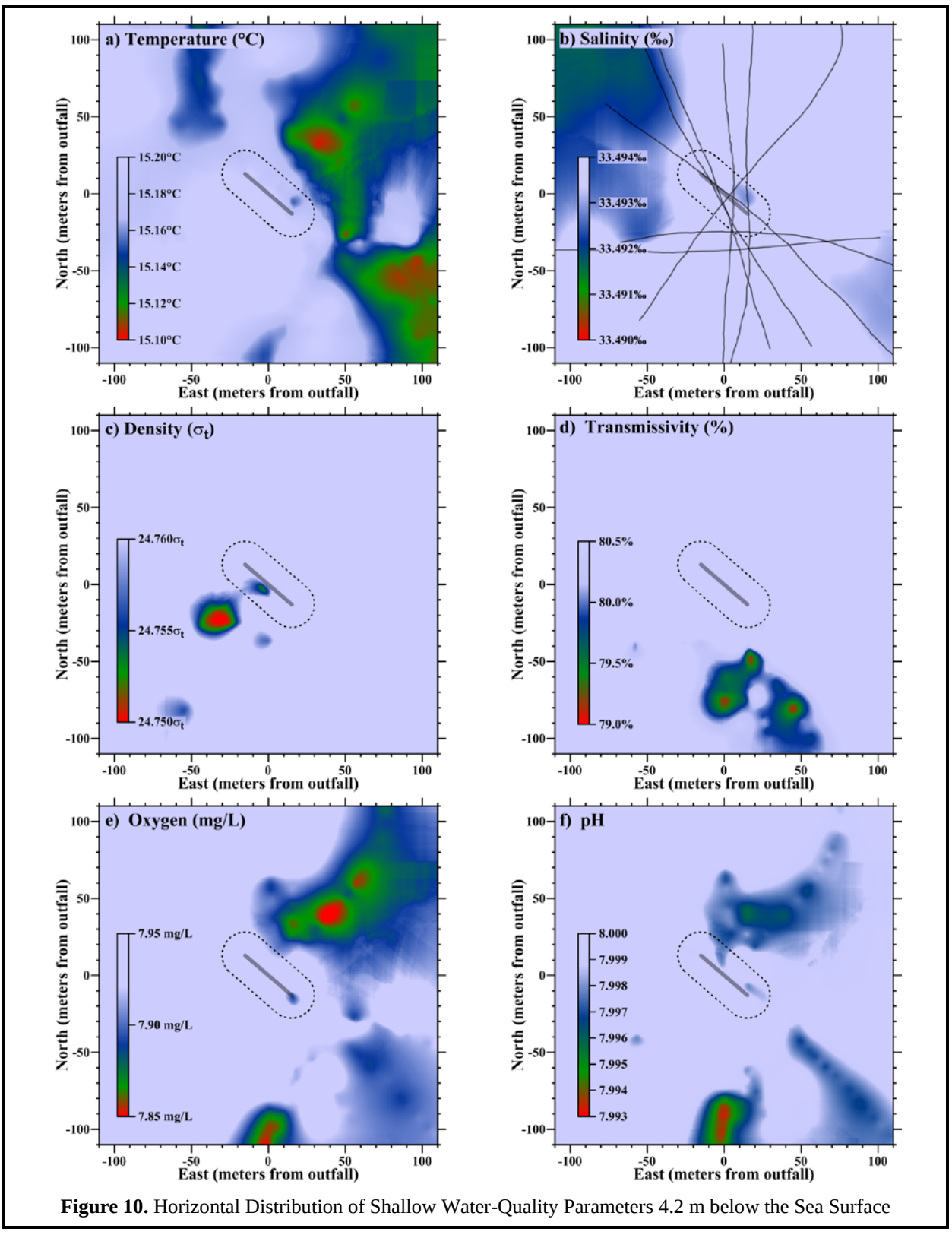

Figure 10. Horizontal Distribution of Shallow Water-Quality Parameters 4.2 m below the Sea Surface

The deep origin of these entrainment-generated anomalies is apparent because the offsets in the upper water column were consistent with the vertical variation in ambient seawater properties that were presented previously in the discussion of vertical profiles in Figure 8. Specifically, temperature, DO, and pH were all naturally lower at near the seafloor where the effluent rapidly entrained the receiving seawater shortly after discharge (red, dark blue, and olive lines in Figure 8). As these deep seawater properties were relocated to the upper water column, they produced the reductions in temperature, DO, and pH (Figure 9aef) that coincided with the plume's salinity anomaly to the west and southwest of the ZID boundary (Figure 9b). Similarly, the increased water clarity (Figure 9d) seen in conjunction with the mid-depth plume arose because the markedly higher transmissivity associated with ambient seawater near a depth of 14 m (light blue lines in Figure 8) was carried upward into the euphotic zone.

The increased transmissivity (less turbidity) and decreased temperature associated with the mid-depth plume signature are particularly diagnostic of anomalies created by the entrainment of bottom seawater; because they could not have been generated by the presence of dilute wastewater constituents. On the day of the survey, the effluent temperature measured onshore prior to discharge was 9°C warmer than that of the receiving seawater at the depth of the mid-depth tow, and therefore, the presence of dilute effluent itself could not have caused the negative (colder) thermal anomaly seen in Figure 9a in conjunction with the plume signature. Instead, entrainment of cold seawater shortly after discharge and its subsequent upward transport by the buoyant plume was the only mechanism that would have created the 0.55 ºC temperature reduction seen in Figure 9a at locations that coincided with the plume's negative salinity anomaly (Figure 9b).

Similarly, the 3.3% increase in transmissivity seen within the plume during the mid-depth tow (blue shaded area west and southwest of the ZID in Figure 9d) could not have been created by the presence of effluent particulates within the discharge plume. Although treated effluent discharged on the day of the survey contained a nominal particulate load (46 mg/L), its turbidity was far greater than that of the receiving seawater. However, as will be demonstrated later in this report, these effluent particulates disperse rapidly shortly after discharge, and thus contribute little to the turbidity of the rising effluent plume.

Instead, transmissivity within the plume was dictated by the properties of ambient seawater entrained immediately above the seafloor, which had a much higher transmissivity (91% near 14 m in the light blue lines of Figure 8) than that of ambient seawater at the depth of the mid-depth tow (82%), where upwelling-induced primary production increased planktonic density. Within the plume at mid-depth, the juxtaposition of the less-turbid bottom seawater entrained within the plume created the region of increased turbidity seen southwest of the diffuser structure in Figure 9d.

It is important to distinguish plume signatures that are caused by the presence of effluent constituents, exemplified by marked reductions in salinity, from those caused by the upward transport of ambient seawater entrained near the seafloor shortly after discharge, embodied by the lateral anomalies in all the other seawater properties associated with the plume at mid-depth. Close to the seafloor, intense mixing is driven by the momentum of the effluent's ejection from the individual diffuser ports. Subsequent turbulent mixing caused by the plume's ascent through the water column is less intense, and as a result, the dilute effluent plume tends to retain the ambient seawater properties it acquired at the seafloor. As in the case of the September 2016 data, these deep seawater properties became apparent as a signature of the buoyant effluent plume when they were juxtaposed against the ambient seawater characteristics in the mid and upper water column. These entrainment-generated anomalies are only apparent, however, when the water column is sufficiently stratified to cause a perceptible contrast between the shallow and deep ambient seawater properties.

The legacies of entrainment anomalies can be particularly long-lived, remaining apparent within the water column well after completion of the initial dilution process. As such, these anomalies provide useful tracers of the diffuse effluent plume during and after the completion of the initial dilution process. However, such anomalies are irrelevant to the receiving-water compliance assessment because the permit restricts attention to water-quality changes caused solely by the presence of wastewater constituents rather than by a simple relocation of ambient seawater.

As with the increased transmissivity found in association with the plume at mid-depth (Figure 9d), the slightly increased density (light blue shading west and southwest of the ZID in Figure 9c) lends insight into the dynamics of the effluent plume in the upper water column. Normally, the rising effluent plume is less dense than the surrounding seawater, and this positive buoyancy indicates that it will continue to rise within the water column. However, the presence of slightly increased density within the plume at mid-depth indicates that that rising plume had overshot its equilibrium depth, and had actually become 'heavier' than the surrounding water. Eventually, the heavy plume would descend slightly in the water column and continue to oscillate vertically in a damped fashion. This indicates that, at the depth of the mid-depth tow, the plume was near buoyant equilibrium, and would remain trapped below the sea surface. At that point, the initial dilution process is assumed complete.

Outfall Performance

The efficacy of the outfall can be evaluated through a comparison of dilution levels measured at the time of the September 2016 survey, and dilutions anticipated from modeling studies that were codified in the discharge permit through limits imposed on effluent constituents. Specifically, the critical initial dilution applicable to the MBCSD outfall was conservatively estimated to be 133:1 (Tetra Tech 1992). That is, dispersion modeling estimated that, at the conclusion of the minimum expected initial mixing, 133 parts of ambient seawater would have mixed with each part of wastewater.

The 133:1 dilution estimate was based on worst-case modeling under highly stratified conditions, where trapping of the plume below a strong thermocline would curtail the additional buoyant mixing normally experienced during the plume's ascent through the entire water column. Additionally, the modeling assumed quiescent oceanic flow conditions, thereby restricting initial mixing processes to the ZID. Under those conditions, the modeling predicted that a 133:1 dilution would be achieved after the plume rose only 9 m from the seafloor, whereupon it would become trapped, ceasing to ascend further in the water column. At that point, the plume would spread laterally with dilution occurring at a much-reduced rate. A 9-m ascent at the MBCSD outfall translates into a trapping depth that is 6.4 m below the sea surface. As described below, however, the dilution levels observed during the September 2016 survey were much higher than the 133:1 predicted by the modeling, even though they were measured at a depth close to the trapping depth predicted by the modeling.

The conservative nature of the critical initial dilution determined from the modeling is an important consideration because it was used to specify permit limitations on chemical concentrations in wastewater discharged from the treatment plant. These end-of-pipe effluent limitations were back calculated from the receiving-water objectives in the COP (SWRCB 2005) using the projected 133-fold dilution determined from the modeling. Application of a higher critical dilution would relax the stringent end-of-pipe effluent limitations thought necessary to meet COP objectives after initial dilution is complete.

End-of-pipe limitations on contaminant concentrations within discharged wastewater were based on the definition of dilution (Fischer et al. 1979). From the mass-balance of a conservative tracer, the concentration of a particular chemical constituent within effluent before discharge (C_e) can be determined from Equation 1.

$$C_e \equiv C_o + D\left(C_o - C_s\right) \qquad \text{Equation 1}$$

where: C_e = the concentration of a constituent in the effluent,
C_o = the concentration of the constituent in the ocean after dilution by D (i.e., the COP receiving-water objective),
D = the dilution expressed as the volumetric ratio of seawater mixed with effluent, and
C_s = the background concentration of the constituent in ambient seawater.

By rearranging Equation 1, the actual dilution achieved by the outfall can be determined from measured seawater anomalies. This measured dilution can then be compared with the critical dilution factor determined from modeling. Salinity is an especially useful tracer because it directly reflects the magnitude of ongoing dilution. The regions of slightly lower salinity apparent west and southwest of the diffuser structure in the mid-depth tow-survey map (Figure 9b), near 11 m in the vertical profiles at Stations RW2 and RW3 north of the ZID (Figure 8bc), and near 6 m in the vertical profile at the southern ZID Station RW4 (Figure 8d), were induced by the presence of dilute wastewater. These salinity anomalies document mixing processes within the effluent plume shortly after discharge, and as it rose through the water column and became trapped at mid-levels of the water column.

The amplitudes of these salinity anomalies quantify the magnitude of wastewater dilution at the various stages of the initial mixing process. By rearranging Equation 1, the dilution ratio (D) can be computed from the salinity anomaly ($A = C_o - C_s$) as:

$$D \equiv \frac{(C_e - C_o)}{\left(C_o - C_s\right)} \propto A^{-1} \qquad \text{Equation 2}$$

The salinity concentration within MBCSD effluent (C_e)[23] is small compared to that of the receiving seawater and, after dilution by more than 133-fold, the salinity of the effluent-seawater mixture is close to ambient salinity. Consequently, to a close approximation, dilution levels are inversely proportional to the amplitude of the salinity anomaly. Thus, a lower effluent dilution at a given location within the effluent plume is directly mirrored by a larger reduction in the measured salinity relative to that of the surrounding seawater.

Among the 9,754 CTD measurements collected during the September 2016 survey, the greatest reduction in salinity (-0.063‰) was recorded during the fifth transect of the mid-depth tow survey when a salinity of 33.429‰ was measured 26 m from the northwestern end of the diffuser structure (red shading in Figure 9b). From Equation 2, the mid-depth salinity anomaly corresponds to a dilution of 512-fold (Figure 11). The salinity reductions seen in the vertical profiles at 11 m at Station RW2 (-0.023‰), at 10.5

[23] Wastewater samples have an average salinity of 0.995‰.

m at Station RW3 (-0.045‰), and between 4 and 6 m at Station RW4 (-0.032‰), were all much smaller. Only the reduction at Station RW3 implied the presence of a marginally perceptible dilution of 722-fold. Thus, all of the measurements collected within the plume during the September 2016 survey greatly exceeded the 133:1 critical initial dilution used to establish limits on contaminant concentrations in wastewater.

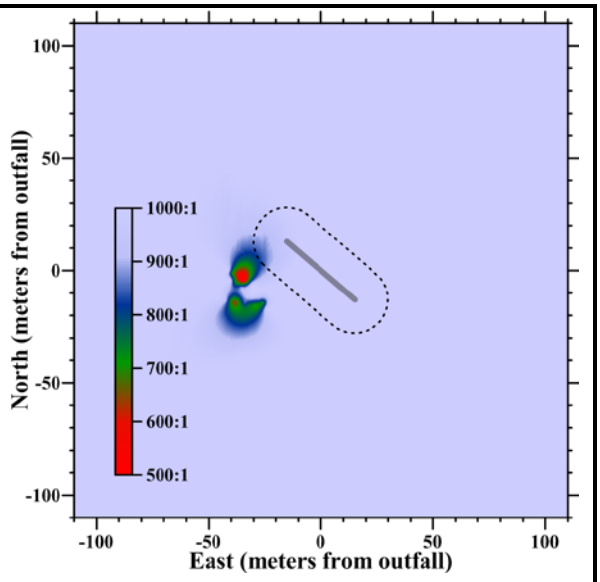

Figure 11. Mid-Depth Plume Dilution Computed from Salinity Anomalies in Figure 9b

In addition, the lowest dilution was measured at a depth of 6.72 m,[24] which close to the 6.4-m trapping depth identified in the modeling that established the 133:1 minimum dilution ratio. According to the conservative modeling results, dilution levels would be expected to be 133:1 at that depth level. Instead, the dilutions were found to be nearly four times greater, indicating that the outfall was dispersing the effluent far more efficiently than predicted by the modeling at the time of the September 2016 survey.

Prior surveys also consistently found dilutions well in excess of the critical initial dilution ratio except very close to a diffuser port and within its turbulent ejection jet. Nearfield measurements within an ejection jet were not collected during the September 2016 survey. Additionally, the lowest dilutions measured at midfield distances during the September 2016 survey were much higher than those found in most other surveys. The uniformly high midfield dilutions observed during the September 2016 survey probably resulted from the increased turbulence generated by the strong vertical shear in the flow field that was described previously in this report. The model used to establish the critical initial dilution ratio specifically excluded the influence of currents that "*flow across the discharge structure.*" Such currents are known to enhance the dilution process markedly, and the vertical shear in the September 2016 flow field undoubtedly contributed to the higher observed dilutions.

Rapid initial dilution associated with the turbulence generated by flow shear also explains why the plume remained trapped at mid-depth during the September 2016 survey, even though the water column was only moderately stratified. Normally, the buoyant effluent plume rises all the way to the sea surface except on rare occasions when the water column is highly stratified. On those occasions, subsurface trapping foreshortens the dilution process and a much lower initial dilution results. Highly stratified conditions were used in the model used to establish the critical initial dilution of 133:1. However, the rapid turbulent dispersion associated with sheared flow both enhances the dilution ultimately achieved within the plume at the completion of the initial dilution process, and causes the plume to rapidly lose its buoyancy by entraining more of the dense ambient seawater at depth. As a result of this rapid buoyancy loss near the seafloor, the plume reaches equilibrium at mid-depth where it remains trapped beneath the sea surface.

[24] During this portion of the fifth mid-depth transect, the CTD was tracking at a slightly shallower depth than the average 7.2 m reported for the entire tow.

Overall, the dilution computations show that, during the September 2016 survey, the outfall was performing better than designed and was rapidly entraining seawater that resulted in dilutions levels exceeding 500-fold even though the plume remained trapped beneath the sea surface. At that location, effluent dilution was considerably higher than the 133:1 critical initial dilution used to establish end-of-pipe permit limitations on contaminant concentrations within wastewater discharged from the MBCSD treatment plant. This demonstrates that, during the September 2016 survey, the COP receiving-water objectives were being easily met by the limits on chemical concentrations within discharged wastewater that are promulgated by the NPDES discharge permit issued to the MBCSD.

COMPLIANCE

This section evaluates compliance with the water-quality limitations listed in the NPDES permit (Table 6). The limits themselves are based on criteria in the COP, the Central Coast Basin Plan, and other state and federal policies that were designed to protect marine life and beneficial uses of ocean waters. Because the limits only pertain to changes in water properties that are caused by the presence of wastewater constituents beyond the ZID, instrumental measurements undergo a series of screening procedures prior to numeric comparison with the permit thresholds. Specifically, the quantitative analyses described in this section focus on water-property excursions caused by the presence of wastewater constituents beyond the ZID, whose amplitudes can be reliably discerned against the backdrop of ambient fluctuations. A detailed understanding of ambient seawater properties, and their natural variability within the region surrounding the outfall, is therefore an integral part of the compliance evaluation presented in this section.

Table 6. Permit Provisions Addressed by the Offshore Receiving-Water Surveys

Limit #	Limit
P1	Floating particles or oil and grease to be visible on the ocean surface
P2	Aesthetically undesirable discoloration of the ocean surface
P3	Temperature of the receiving water to adversely affect beneficial uses
P4	Significant reduction in the transmittance of natural light at any point outside the ZID
P5	The DO concentration outside the zone of initial dilution to fall below 5.0 mg/L or to be depressed more than 10% from that which occurs naturally
P6	The pH outside the zone of initial dilution to be depressed below 7.0, raised above 8.3, or changed more than 0.2 units from that which occurs naturally

The results of these analyses of the September 2016 data demonstrate that the MBCSD discharge complied with the NPDES discharge permit. Moreover, although observations within the ZID are not subject to compliance evaluations, they met the prescribed limits because actual dilution levels routinely exceeded the conservative design specifications assumed in the discharge permit. Thus, the quantitative evaluation described in this section documents an outfall and treatment process that was performing at a high level during the September 2016 survey.

Permit Provisions

The offshore receiving-water surveys are designed to assess compliance with objectives dealing with undesirable alterations to six physical and chemical characteristics of seawater. Specifically, the permit states that wastewater constituents within the discharge shall not cause the limits listed in Table 6 to be exceeded.

The first two receiving-water limits, P1 and P2, rely on qualitative visual observations for compliance evaluation. Compliance was demonstrated during the September 2016 survey through visual inspection of the sea surface that found an absence of floating wastewater materials, oil, grease, and discoloration of the sea surface.

Compliance with the remaining four receiving-water limitations is quantitatively evaluated through a comparison between instrumental measurements and numerical limits listed in the NPDES permit. For example, in P5 and P6, the fixed numeric limits on absolute values of DO (>5 mg/L) and pH (7.0 to 8.3) can be directly compared with field measurements within the dilute wastewater plume beyond the ZID. However, both P5 and P6 also contain narrative limits, which originate in the COP, and define unacceptable water-quality impacts in terms of "*significant*" excursions beyond those that occur "*naturally*." Quantitative evaluation of these limits requires a further comparison of field measurements with numerical thresholds that reflect the natural variation in transmissivity, DO, and pH within the receiving waters surrounding the outfall.

As described previously, natural variation in seawater properties can result from a variety of oceanographic processes. These processes establish the range in ambient seawater properties caused by natural spatial variation within the survey region at a given time (e.g., vertical stratification), and by temporal variations caused by seasonal and interannual influences (e.g., El Niño and La Niña). Of particular interest are upwelling and downwelling processes that not only determine average properties at a given time, but also the degree of water-column stratification, or spatial variability, present during any given survey.

Screening of Measurements

Evaluating whether any of the 9,754 CTD measurements collected during the September 2016 survey exceeded a permit limit can be a complex process. For example, although apparently significant excursions in an individual seawater property may be related to the presence of wastewater constituents, they may also result from instrumental errors, natural processes, entrainment of ambient bottom waters in the rising effluent plume, statistical uncertainty, ongoing initial mixing within and beyond the ZID, or other anthropogenic influences (e.g., dredging discharges or oil spills).

Because of this complexity, measurements were first screened to determine whether numerical limits on individual seawater properties apply (Table 7). The screening procedure sequentially applies three questions to restrict attention to: 1) the oceanic area where permit provisions pertain; 2) changes due to the presence of wastewater particulates; and 3) changes large enough to be reliably detected against the backdrop of natural variation. The measurements that remain after completing the screening process can then be compared with Basin-Plan numerical limits and COP allowances.

The following subsection provides additional lines-of-evidence that demonstrate compliance with numerical permit limits independent of the screening process. The rationale for identifying observations suitable for further compliance analysis is presented in the following descriptions of the three screening steps.

1. Measurement Location: The COP states that compliance with its receiving-water objectives "*shall be determined from samples collected at stations representative of the area within the waste field where initial dilution is completed.*" Initial dilution includes the mixing that occurs from the turbulence associated with both the ejection jet, and the buoyant plume's subsequent ascent through the water column.

Table 7. Receiving-Water Measurements Screened for Compliance Evaluation

Topic Addressed	Screening Question	Answer No	Answer Yes[25]	*Parameter*
Location	1. Was the measurement collected beyond the 15.2-m ZID boundary where modeling assumes that initial dilution is complete?	*1,073*	*8,681*	All
Wastewater Constituents	2. Did the beyond-ZID measurement coincide with a quantifiable salinity anomaly (≤550:1 dilution level) indicating the presence of detectable wastewater constituents?	*8,677*	*4*	All
Natural Variation	3. Did seawater properties associated with the wastewater measurements depart significantly from the expected range in ambient seawater properties at the time of the survey?	*4*	*0*	Temperature
		4	*0*	Transmissivity
		4	*0*	DO
		4	*0*	pH

Although currents often transport the plume well beyond the ZID before the initial dilution process is complete, the COP states that dilution estimates shall be based on "*the assumption that no currents, of sufficient strength to influence the initial dilution process, flow across the discharge structure.*" Because of this, the regulatory mixing distance, which is equal to the 15.2-m water depth of the discharge, provides a conservative boundary to screen receiving-water data for subsequent compliance evaluation. Application of this initial screening question to the September 2016 dataset eliminated 1,073 of the original 9,754 receiving-water observations from further consideration because they were collected within the ZID (Table 7, Question 1). The remaining 8,681 observations were carried forward in the screening analysis.

2. Presence of Wastewater Constituents: The MBCSD discharge permit restricts application of the numerical receiving-water limits to excursions caused by the presence of wastewater constituents. This confines the compliance analysis to changes caused "*as the result of the discharge of waste*," as specified in the COP, rather than anomalies that arise from the upward movement of ambient seawater entrained within the buoyant effluent plume. Analyses conducted on quarterly receiving-water surveys over the last decade have demonstrated that the direct influence of dilute wastewater is almost never observed in any seawater property other than salinity, except very close (<1 m) to a diffuser port and within its ejection jet.

In fact, negative salinity anomalies are the only consistent indicator of the presence of wastewater constituents within receiving waters. Wastewater salinity is negligible compared to that of the receiving seawater, so the presence of a distinct salinity minimum provides *de facto* evidence of the presence of wastewater constituents. Because of the large contrast between the nearly fresh wastewater and the salty receiving water, salinity provides a powerful tracer of dilute wastewater that is unrivaled by other seawater properties. Other properties do not exhibit such a large contrast and, as such, their wastewater signatures dissipate rapidly upon discharge with very little mixing. Wastewater's lack of salinity, however, provides a definitive tracer that allows the presence of effluent constituents to be identified even after dilution many times greater than the 133-fold critical initial dilution assumed in the discharge permit.

[25] Number of remaining CTD observations of potential compliance interest based on sequential application of each successive screening question

As described in the previous section, wastewater-induced reductions in salinity can be used to determine the amount of dilution achieved by initial mixing. Based on statistical analyses of the natural variability in salinity readings measured near the outfall over a five-year period between 2004 and 2008, the smallest reduction in salinity that can be reliability detected within receiving waters is 0.062‰. This represents a dilution level of 542-fold in Equation 2. Salinity reductions that are smaller than 0.062‰ cannot be reliably discerned against the backdrop of natural variation, and would not result in discernible changes in other seawater properties. Eliminating those measurements from further evaluation restricts attention to excursions in temperature, light transmittance, DO, and pH that are potentially related to the presence of wastewater constituents.

As discussed previously, the greatest salinity reduction observed during the September survey was recorded southwest of the diffuser structure during the mid-depth tow survey. Additional marginal reductions possibly associated with more dilute portions of the plume were measured beyond the northern boundary of the ZID during vertical profiling at Station RW2 and RW3, and within the vertical profile immediately south of the ZID boundary at Station RW4. However, only four of the salinity reductions were large enough to be reliably determined against the backdrop of natural variability (Table 7). All were measured during the mid-depth tow, and were associated with dilutions ranging from 512-to-536-fold. Other salinity measurements corresponded to dilutions less than 550:1. In particular, 8,677 observations that were measured outside the ZID during the September 2016 survey did not have salinity reductions that were greater than the 0.062‰ plume-detection threshold.

3. Natural Variation: An integral part of the compliance analysis is determining whether a particular anomalous measurement resulted from the presence of wastewater constituents, or whether it simply became apparent because ambient seawater was relocated (upward) by the plume. If the measurement does not significantly depart from the natural range in ambient seawater properties at the time of the survey, then it is difficult to ascribe the departure to the presence of wastewater constituents. Thus, quantifying the natural variability around the outfall at the time of the survey is necessary for determining whether a particular observation warrants comparison with the numeric permit limits.

A statistical analysis of receiving-water data collected around the outfall was used to establish the range in natural conditions surrounding the outfall (first three data columns of Table 8). These ambient-variability ranges were used to identify significant departures from natural conditions that could be indicative of adverse discharge-related effects on water quality. The same five-year database used to establish the within-survey salinity variation discussed previously, was also used to establish one-sided 95% confidence bounds on transmissivity (-10.2%), temperature (+0.82°C), DO (-1.38 mg/L), and pH (± 0.094). These were combined with 95^{th} percentiles determined from the September 2016 ambient seawater data, to establish time-specific natural-variability thresholds in a manner analogous to COP Appendix VI. The percentiles were largely determined from September 2016 vertical profile data collected at Stations RW1, RW5, and RW6, and excluded measurements potentially affected by the discharge.

Temperature, transmissivity, pH, and DO concentrations associated with the four remaining measurements of potential compliance interest were all well within their respective ranges of natural variability (Table 7, Question 3). As such, the screening process unequivocally eliminated all of the measurements collected during the September 2016 survey from further consideration in the compliance analysis. In fact, all of the documented excursions in these properties were the result of physical processes unrelated to the presence of wastewater constituents, namely, entrainment of near-bottom seawater within the rising effluent plume.

Table 8. Compliance Thresholds

Water Quality Property	95% Confidence Bound[26]	95th Percentile[27,28]	Natural Variability Threshold[29]	COP Allowance[30]	Basin Plan Limit[31]	Extremum[32]
Temperature (ºC)	0.82	15.39	>16.21	—	—	≤15.45
Transmissivity (%)	-10.2	81.0	<70.8	—	—	≥78.8
DO (mg/L)	-1.38	6.72	<5.34	<4.81	<5.00	≥6.70
pH (minimum)	-0.094	7.958	<7.864	<7.664	<7.000	≥7.941
pH (maximum)	0.094	8.035	>8.129	>8.329	>8.300	≤8.037

As described previously, anomalies in seawater properties clearly delineated the plume, but those entrainment-generated excursions were not caused by the presence of wastewater constituents. During periods when the water column is even slightly stratified, ambient seawater properties near the seafloor differ from those within the rest of the water column, and their juxtaposition within the rising effluent plume appears as lateral anomalies within the upper water column. Regardless, if the presence of wastewater particulates had contributed to the observed decreases in DO and pH within the upper water column, their influence would still have been well within the natural range of the ambient seawater properties at the time of the survey. Consequently, their influence on water quality would not be considered environmentally significant.

Other Lines of Evidence

Several additional lines of evidence further support the conclusion that all the CTD measurements collected during the September 2016 survey complied with the quantitative permit limits P3 through P6 in Table 6. In combination, these lines of evidence provide the "best explanation" of the origin and significance of individual measurements using abductive inference (Suter 2007). This process, which has been used to implement sediment-quality guidelines for California estuaries (SWRCB 2009), emphasizes a pattern of reasoning that accounts for both discrepancies and concurrences among multiple lines of evidence. A best explanation approach serves to limit the uncertainty associated with each individual

[26] The one-sided confidence bound measures the ability to reliably determine ambient seawater properties within surveys as a whole. They were determined from an analysis of the variability in ambient water-quality data collected during 20 quarterly surveys conducted between 2004 and 2008. Although water-quality observations potentially affected by the presence of wastewater constituents were excluded from the analysis, more than 9,200 remaining observations for each of the six seawater properties accurately quantified the inherent uncertainty in defining the range in natural conditions.

[27] The COP (Appendix I, Page 27, SWRCB 2005) defines a "*significant*" difference as "*a statistically significant difference in the means of two distributions of sampling results at the 95% confidence level*." Accordingly, COP effluent analyses (Step 9 in Appendix VI, Page 42, Ibid.) are based "*the one-sided, upper 95% confidence bound for the 95th percentile*."

[28] The 95th-percentile quantified natural variability in seawater properties during the September 2016 survey itself, and was determined from vertical-profiles data unaffected by the discharge.

[29] Thresholds represent limits on wastewater-induced changes to receiving-water properties that significantly exceed natural conditions as specified in the discharge permit and COP. They are determined from the sum of columns to the left and are specific to the September 2016 survey. They do not include the COP allowances specified in the column to the right.

[30] The discharge permit, in accordance with the COP, allows excursions in seawater properties that depart from natural conditions by specified amounts. DO cannot be "*depressed more than 10% from that which occurs naturally*," and pH cannot be "*changed more than 0.2 units from that which occurs naturally.*"

[31] Permit limits P5 and P6 (Table 6) include specific numerical values promulgated in the RWQCB Basin Plan (1994) in addition to changes relative to natural conditions specified in the COP. The Basin Plan upper-bound pH objective for ocean waters is 8.5, but a more-stringent upper-bound objective of 8.3, which applies to individual beneficial uses, was implemented in the MBCSD discharge permit.

[32] Maximum or minimum value measured during the September 2016 survey, regardless of location within or beyond the ZID

CTD measurement, and to provide a more robust compliance assessment. Together, these lines of evidence significantly strengthen the conclusion that the discharge fully complied with the permit at the time of the September 2016 survey.

Insignificant Thermal Impact: Although there are no explicit numerical objectives for discharge-related increases in temperature, a numerical limit can be established for thermal excursions that is based on the requirement that they not adversely affect beneficial uses (P3 in Table 6). Increases in temperature caused by the discharge of warm wastewater could be deemed to affect beneficial uses adversely if they exceeded the natural temperature range observed at the time of the survey (i.e. exceeded 16.21°C listed in the third data column of Table 8). However, none of the 9,754 CTD measurements collected during the September 2016 survey exceeded 15.45°C (last column in Table 8). Additionally, as mentioned previously, because the effluent entrained cooler bottom water shortly after discharge, the rising plume actually exhibited a lower temperature than the surrounding seawater in the upper water column (Figure 9a).

Limited Ambient Light Penetration: As with temperature, there are no explicit numerical objectives for discharge-related decreases in transmissivity. However, the COP narrative objective (P4) limiting significant reductions in the transmission of natural light can also be translated into a numerical objective. Specifically, because the COP does not specify an allowance beyond natural conditions, the same 70.8% threshold on ambient transmissivity variations listed in third data column of Table 8 can be interpreted to constitute a numerical limit.

However, none of the transmissivity measurements collected during the September 2016 survey fell below the 70.8% minimum compliance threshold. The lowest transmissivity (78.83%) was recorded during the shallow tow at a location 75 m south of the diffuser structure and well beyond the influence of the discharge (red shading in Figure 10d). In fact, during the September 2016 survey, transmissivity was uniformly low throughout the upper water column (light blue lines above 8 m in Figure 8). As described previously, this increased turbidity (reduced transmissivity) within the upper water column was a natural consequence of upwelling, namely, enhancement of primary production by the upward transport of nutrients into the euphotic zone.

Moreover, the COP objective for light penetration only applies to a portion of the transmissivity measurements. Because little natural light is present beneath the euphotic zone, which extends to approximately twice the Secchi depth, the limit on transmissivity reductions during the September 2016 survey only applies to measurements recorded above 10 m (twice the average Secchi depth listed in Table 4). Consequently, even if the discharge of wastewater particulates had caused transmissivity measurements collected below the euphotic zone to drop below the numeric compliance threshold, it would not have been of regulatory concern because the penetration of ambient light would not have been affected. This includes measurements collected within the naturally turbid BNL above the seafloor where virtually no natural light was present during the September 2016 survey.

Directional Offset: Analysis of the directional offset of CTD measurements is useful because wastewater and receiving-seawater properties depart from one another in several predictable ways. Specifically, upon discharge, wastewater is fresher, warmer, and lighter than the ambient receiving waters of Estero Bay. Under most conditions, wastewater is also more turbid than the receiving waters because of organic particulates suspended in the treated effluent. As such, the presence of wastewater constituents will reduce the salinity, density, and transmissivity of the receiving seawater (negative offset), while temperature will be increased (positive offset). Therefore, as discussed previously, the reduced temperatures observed in conjunction with the effluent plume during the mid-depth tow (Figure 9a) could not have been generated by the presence of warmer wastewater constituents. Similarly, the increased transmissivity observed within the discharge plume at that same location (Figure 9d) could not have been

generated by an unacceptably high particulate load within wastewater. In both cases, the directional offsets were opposite of receiving-water impacts expected from the presence of wastewater constituents.

Insignificant Wastewater Particulate Loads: Another independent line of evidence demonstrates that the discharge of wastewater particulates could not have contributed materially to turbidity within the dilute effluent plume. The suspended-solids concentration measured onshore, within the effluent, and immediately prior to discharge from the WWTP on 20 September 2016 was 46 mg/L. After dilution by at least 512-fold, the effluent suspended-solids concentration would have the reduced ambient transmissivity by no more than 0.7%. This small potential decrease in transmissivity is overwhelmed by the large 9.5% decrease in ambient transmissivity caused by the increased presence of plankton within the euphotic zone caused by upwelling.

Similarly, the MBCSD discharge could not have contributed materially to the observed DO fluctuations. The MBCSD treatment process routinely removes 80% or more of the organic material, as demonstrated by the low, 45-mg/L BOD measured within the plant's effluent three days after the survey. That small amount of BOD would have induced a DO depression of no more than 0.022 mg/L after dilution (MRS 2002). In fact, in the absence of tangible BOD influence, wastewater discharge would actually be expected to increase DO within subsurface receiving waters, rather than decrease it. This is because effluent is oxygenated by recent contact with the atmosphere during the treatment process, whereas receiving waters at depth are typically depleted in DO due to the long absence of atmospheric equilibration within the deep offshore watermass.

COP Allowances: The COP does not explicitly require that wastewater-induced changes remain within the ranges in natural variation listed in the third data column of Table 8, even though these ranges were conservatively used in the data screening process described in previous subsections. Consideration of these COP allowances for receiving-water limits provides an additional safety factor in the compliance evaluation.

For pH, the COP and the discharge permit allow changes up to 0.2 pH units from natural conditions, bringing the minimum allowed pH down to 7.664 during the September 2016 survey (fourth data column of Table 8). This limiting value is significantly less than the lowest pH measurement of 7.941 recorded during the September 2016 survey (last column of Table 8).[33] Similarly, the lowest DO concentration measured during the survey (6.70 mg/L) was well above both the lower range in natural variation (5.34 mg/L) and the 10% compliance threshold promulgated by the COP (4.81 mg/L).

Excursions remained within the fixed Basin-Plan Limits: Permit provisions P5 and P6 (Table 6) combine receiving-water objectives from both the COP and the Basin Plan with regard to DO and pH limits. As described previously, the COP requires that DO concentrations outside the ZID not be depressed more than 10% from that which occurs naturally, and restricts pH measurements to those within 0.2 units of that which occurs naturally. In contrast, the Basin-Plan's fixed numerical limits do not provide specific guidance as to how they might change in response to widespread changes in oceanographic conditions unrelated to the discharge. Specifically, the fixed numerical limits restrict DO concentrations outside the ZID to no less than 5 mg/L (P5 in Table 6), and pH levels to the 7.0-to-8.3 range (P6). As such, the fixed Basin-Plan limit on DO is slightly more restrictive than the 4.81 mg/L minimum allowable DO concentration established for the September 2016 survey under COP objectives; yet the all of the DO measurements also complied with the more conservative Basin-Plan limit on DO reductions. Similarly, the minimum allowable pH (7.0) specified in the Basin Plan was more restrictive

[33] Compliance with COP maximum pH allowance (8.329) is irrelevant because effluent on the day of the survey had a pH of 7.4, which is much lower than the lowest pH measured within the receiving seawater (7.941). Consequently, the presence of effluent constituents could not have induced an increase in pH within receiving waters.

than the COP limits (7.664) specified for the September 2016 Survey, yet all the measurements again complied with both regulations.

Natural Variability within and beyond the ZID: Although the permit limits only apply to changes in DO, pH, temperature, and transmissivity beyond the ZID, examination of measurements acquired within the ZID frequently provides additional insight into the potential for adverse effects on water quality. However, among all the data collected during the September 2016 survey, salinity was the only seawater property that exhibited a perceptible difference from ambient conditions. Regardless of their association with the plume's effluent salinity signature or their proximity to the diffuser structure, none of the 9,754 temperature, DO, pH, and transmissivity observations exceeded the thresholds of natural variability, or the Basin-Plan limits specified in Table 8.

CONCLUSIONS

The quantitative screening analysis demonstrated that all measurements recorded during the September 2016 survey complied with the receiving-water limitations specified in the NPDES discharge permit. This conclusion was further strengthened by other lines of evidence supporting compliance with the discharge permit. Specifically, although discharge-related changes in seawater properties were observed during the September 2016 survey, the changes were either not of significant magnitude (i.e., they were within the natural range of variability that prevailed at the time of the survey), were measured within the boundary of the ZID where initial mixing is still expected to occur, or were not directly caused by the presence of wastewater constituents within the water column (i.e., were entrainment generated).

Even though the plume became trapped well beneath the sea surface at the completion of the initial dilution process, turbulence generated by shear in the flow field allowed effluent to achieve dilution levels above 512-fold, which is far in excess of the 133-fold critical initial dilution level predicted by design modeling. Within the zone of turbulent counterflow below the trapping depth, only marginally perceptible reductions in salinity, reflecting dilution levels above 722-fold, were found at Station RW3 along the northern boundary of the ZID, and in a direction opposite of the mid-depth flow measured by the drogued drifter. All of the measured dilution levels far exceeded levels that were predicted by modeling and that were incorporated in the discharge permit as limits on contaminant concentrations within effluent prior to discharge. Lastly, all of the auxiliary observations collected during the September 2016 survey demonstrated that the discharge complied with the narrative receiving-water limits in the discharge permit and the COP. Together; these observations demonstrate that the treatment process, diffuser structure, and the outfall continue to surpass design expectations.

REFERENCES

Davis, R.E., J.E. Dufour, G.J. Parks, and M.R. Perkins. 1982. Two Inexpensive Current-Following Drifters. Scripps Institution of Oceanography, University of California, San Diego, La Jolla, California. SIO Reference No. 82-28. December 1982.

Fischer, H.B., E.J. List, R.C.Y. Koh, J. Imberger, and N.H. Brooks. 1979. Mixing in Inland and Coastal Waters. New York: Academic Press, 482 p.

Kuehl, S.A., C.A. Nittrouer, M.A. Allison, L. Ercilio, C. Faria, D.A. Dukat, J.M. Jaeger, T.D. Pacioni, A.G. Figueiredo, and E.C. Underkoffler 1996. Sediment deposition, accumulation, and seabed dynamics in an energetic fine-grained coastal environment. *Continental Shelf Research*, 16: 787-816.

Marine Research Specialists (MRS). 1998. City of Morro Bay and Cayucos Sanitary District, Offshore Monitoring and Reporting Program, Semiannual Benthic Sampling Report, April 1998 Survey. Prepared for the City of Morro Bay, CA. July 1998.

Marine Research Specialists (MRS). 2002. City of Morro Bay and Cayucos Sanitary District, Supplement to the 2002 Renewal Application For Ocean Discharge Under NPDES Permit No. Prepared for the City of Morro Bay and Cayucos Sanitary District, Morro Bay, CA. July 2002.

Marine Research Specialists (MRS). 2011. City of Morro Bay and Cayucos Sanitary District, Offshore Monitoring and Reporting Program, 2010 Annual Report. Prepared for the City of Morro Bay, California. March 2011.

Marine Research Specialists (MRS). 2012. City of Morro Bay and Cayucos Sanitary District, Offshore Monitoring and Reporting Program, 2011 Annual Report. Prepared for the City of Morro Bay, California. March 2012.

Marine Research Specialists (MRS). 2013. City of Morro Bay and Cayucos Sanitary District, Offshore Monitoring and Reporting Program, 2012 Annual Report. Prepared for the City of Morro Bay, California. March 2013.

Marine Research Specialists (MRS). 2014. City of Morro Bay and Cayucos Sanitary District, Offshore Monitoring and Reporting Program, 2013 Annual Report. Prepared for the City of Morro Bay, California. March 2014.

National Academy of Sciences. 1993. Managing Wastewater in Coastal Urban Areas. National Research Council Committee on Wastewater Management for Coastal Urban Areas, Water Science and Technology Board, Commission on Engineering and Technical Systems. 477 pp.

Regional Water Quality Control Board (RWQCB) - Central Coast Region. 1994. Water Quality Control Plan (Basin Plan) Central Coast Region. Available from the RWQCB at 81 Higuera Street, Suite 200, San Luis Obispo, California. 148p. + Appendices.

Regional Water Quality Control Board (RWQCB) - Central Coast Region and the Environmental Protection Agency (USEPA) – Region IX. 1992a. Waste Discharge Requirements (Order No. 92-67) and Authorization to Discharge under the National Pollutant Discharge Elimination System (Permit No. CA0047881) for City of Morro Bay and Cayucos Sanitary District, San Luis Obispo County.

Regional Water Quality Control Board (RWQCB) - Central Coast Region and the Environmental Protection Agency (USEPA) – Region IX. 1992b. Monitoring and Reporting Program No. 92-67 for City of Morro Bay and Cayucos Sanitary District, San Luis Obispo County (Permit No. CA0047881).

Regional Water Quality Control Board (RWQCB) - Central Coast Region and the Environmental Protection Agency (USEPA) – Region IX. 1998a. Waste Discharge Requirements (Order No. 98-15) and National Pollutant Discharge Elimination System (Permit No. CA0047881) for City of Morro Bay and Cayucos Sanitary District, San Luis Obispo County. 11 December 1998.

Regional Water Quality Control Board (RWQCB) - Central Coast Region and the Environmental Protection Agency (USEPA) – Region IX. 1998b. Monitoring and Reporting Program No. 98-15 for City of Morro Bay and Cayucos Sanitary District, San Luis Obispo County. 11 December 1998.

Regional Water Quality Control Board (RWQCB) - Central Coast Region and the Environmental Protection Agency (EPA) – Region IX. 2009. Waste Discharge Requirements (Order No. R2-2008-0065) and National Pollutant Discharge Elimination System (Permit No. CA0047881) for the Morro Bay and Cayucos Wastewater Treatment Plant Discharges to the Pacific Ocean, Morro Bay, San Luis Obispo County. Effective 1 March 2009.

Sea-Bird Electronics, Inc. (SBE) 1989. Calculation of M and B Coefficients for the Sea-Tech Transmissometer. Application Note No. 7, Revised September 1989.

Sea-Bird Electronics, Inc. (SBE) 1992. SBE 12/22/22/20 Dissolved Oxygen Sensor Calibration and Deployment. Application Note No. 12-1, rev B, Revised April 1992.

Southern California Bight Field Methods Committee (SCBFMC). 2002. Field Operation Manual for Marine Water-Column, Benthic, and Trawl monitoring in Southern California. Technical Report 259. Southern California Coastal Water Research Project. Westminster, CA. March 2002.

State Water Resources Control Board (SWRCB). 2005. Water Quality Control Plan, Ocean Waters of California, California Ocean Plan. California Environmental Protection Agency. Effective February 14, 2006.

State Water Resources Control Board (SWRCB). 2009. Water Quality Control Plan for Enclosed Bays and Estuaries – Part 1 Sediment Quality. California Environmental Protection Agency. Effective August 22, 2009. sed_qlty_part1.pdf [Accessed 02/26/10].

Suter II, Glenn, W. 2007. Ecological risk assessment, 2nd edition. U. S. Environmental Protection Agency, Cincinnati, Ohio. CRC.

Tetra Tech. 1992. Technical Review City of Morro Bay, CA Section 201(h) Application for Modification of Secondary Treatment Requirements for a Discharge into Marine Waters. Prepared for the U.S. Environmental Protection Agency, Region IX, San Francisco, CA by Tetra Tech, Inc., Lafayette, CA. February 1992.